

# Evaluating the Performance of Fiber-Based Concrete Mixes for Various Applications

**Project Leader:** Surya Sarat Chandra Congress

**Team Members:** Krishneswar Ramineni, Akash Ashok  
Tanshette, Nripojyoti Biswas

**PI:** Anand J. Puppala

Professor | A.P. and Florence Wiley Chair

Director – Center for Infrastructure Renewal

Closed Meeting

TAMU Site Proprietary

NSF IUCRC CICI TAMU SITE  
NSF IUCRC CICI - IAB Spring 2023 Meeting

# Presentation Outline

- ❖ **Introduction**
  - ❖ **Objectives**
  - ❖ **Progress of Work**
  - ❖ **Laboratory Testing**
  - ❖ **Results**
  - ❖ **Observations**
  - ❖ **Future Work**
- 

# Introduction

- ❖ **Climate change and rising seawater levels → huge concerns for coastal areas**
- ❖ **Increase in intensity of storm surges → coastal areas are vulnerable**
  - ❑ **Coastal flooding**
  - ❑ **Water pollution**
  - ❑ **Shoreline erosion**
  - ❑ **High salinity of coastal waters**



A neighborhood in Port Arthur, Texas, flooded by Hurricane Harvey in 2017\*<sup>a</sup>



Floods from Hurricane Ian, Naples, Florida, USA September 2022\*<sup>b</sup>

# Introduction

- ❖ Sandbags are used as barriers to control the destructive behavior of flooding

- ❖ Limitations of the current methods

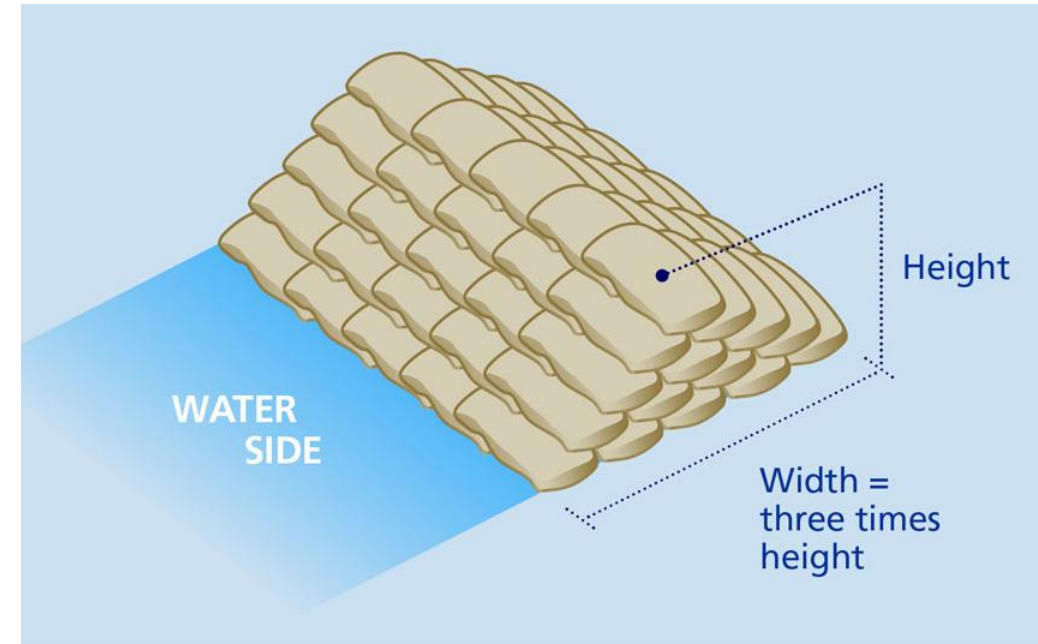
- Handling and logistical issues

- Long-term performance of sandbags

- Limited resources

- ❖ Objective

- To develop optimized fiber-based concrete mixes to address the flooding and erosion-related coastal infrastructure problems caused due to climate change



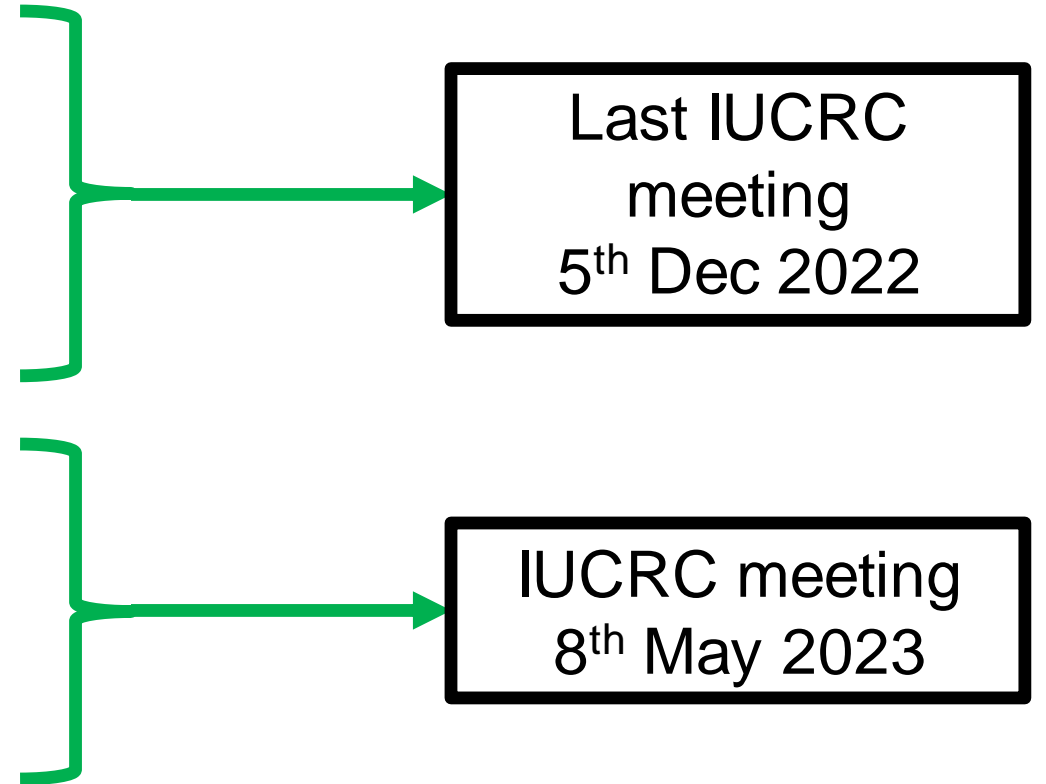
\*Source: [www.zurich.com](http://www.zurich.com)

Typical schematic of sandbagging method\*

# Progress of Work

## Task List

- ❖ **Characterization of materials**
- ❖ **Wetting and Drying studies**
  - ❑ **Potable water (4°C, 20°C and 40°C)**
  - ❑ **Seawater (4°C and 20°C)**
- ❖ **Permeability studies**
- ❖ **Strength studies**
- ❖ **Laboratory-scale large box studies**



Last IUCRC  
meeting  
5<sup>th</sup> Dec 2022

IUCRC meeting  
8<sup>th</sup> May 2023

# Laboratory Testing

## Concrete mix proportion

Percentage	60%	50%	40%	30%	control
Proportions	1:3:3:10.5	1:3:3:7	1:3:3:4.67	1:3:3:3	1:3:3:0
Cement (g)	86.3	107.8	129.4	151.0	215.7
Sand (g)	322.1	402.6	483.0	563.6	805.2
Pea Gravel (g)	296.2	370.3	444.2	518.4	740.6
Fiber (g)	135.9	113.2	90.6	67.9	0

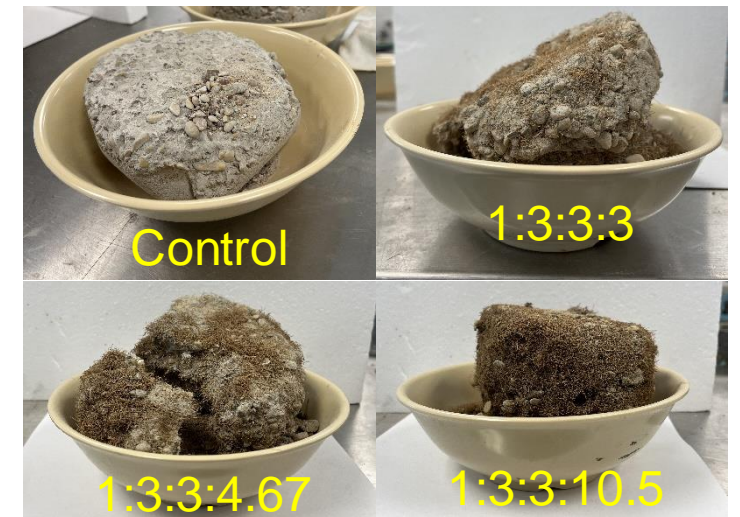
\*Note - Proportions A:B:C:D = Cement: Fine aggregate: Coarse aggregate: Fibers



Concrete mix constituents



Concrete mixes during wetting and drying cycles



Concrete mixes after five wetting and drying cycles at 20 C

# Laboratory Testing

## Permeability studies

- ❖ Hydraulic conductivity of the concrete mixes was measured as per ASTM D5084
- ❖ Falling Head method was used
- ❖ Sample size: 6-inch dia and 2.5-inch height

$$k = 2.303 \frac{aL}{At} * \frac{h_1}{h_2}$$

Where,  $k$  = Hydraulic conductivity

$a$  = Cross section area of standpipe

$A$  = Cross section area of sample

$L$  = Height of sample

$h_1, h_2$  = head before and after test



Dry concrete mixes samples in molds



Permeability test setup

# Laboratory Testing

## Compressive strength tests

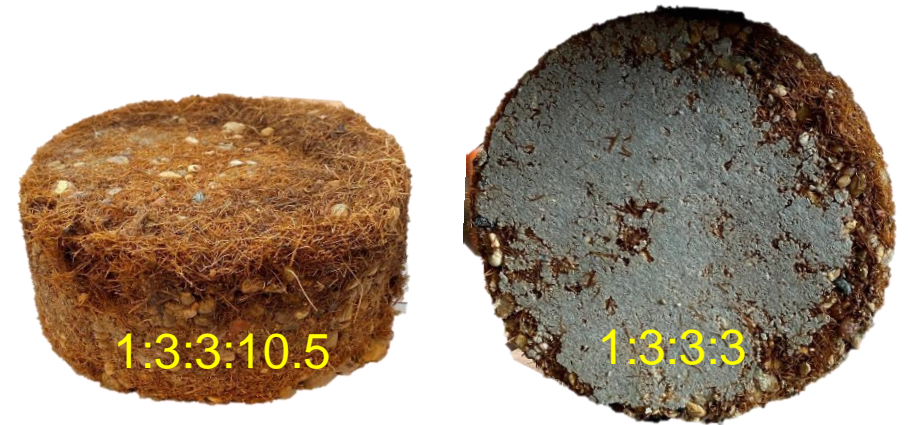
- ❖ Compressive strength testing was performed as per ASTM D2166
- ❖ Sample size: 2-inch dia and 4-inch height
- ❖ Strain rate: 1% per minute



Compressive strength sample preparation

## Split Tensile strength tests

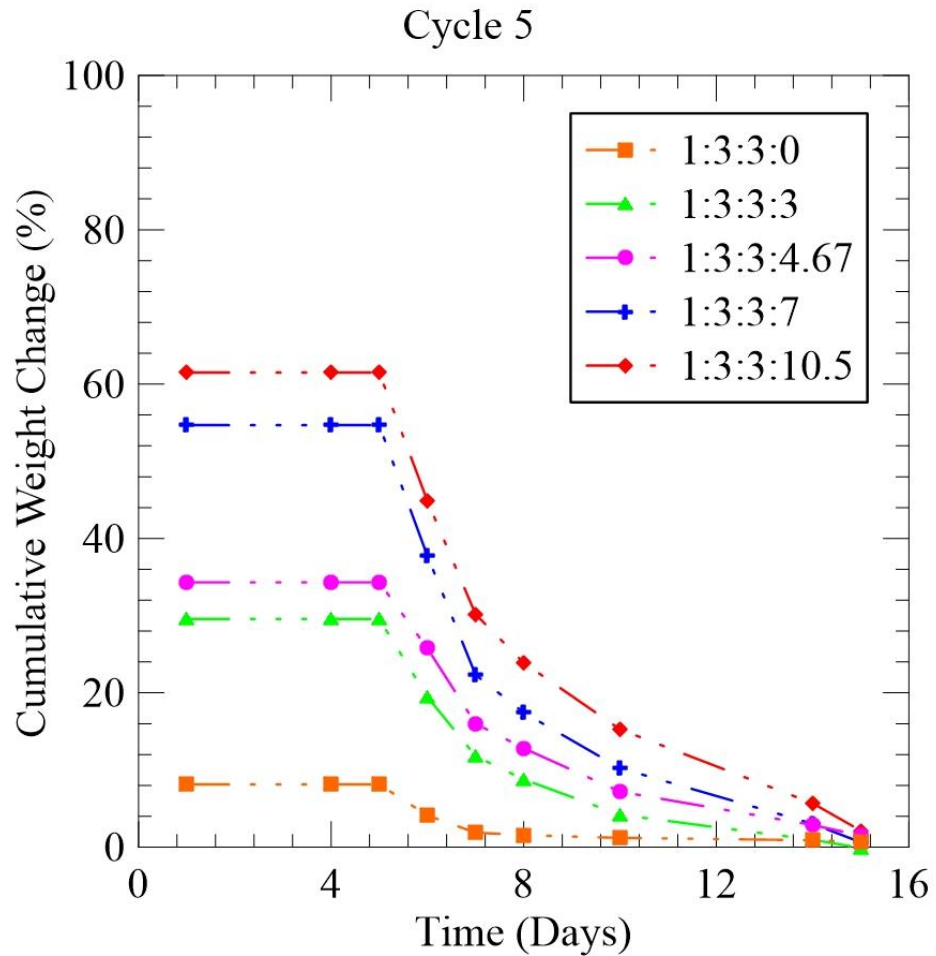
- ❖ Split tensile strength was performed on 6-inch dia and 2.5-inch height sample
- ❖ Strain rate: 1% per minute



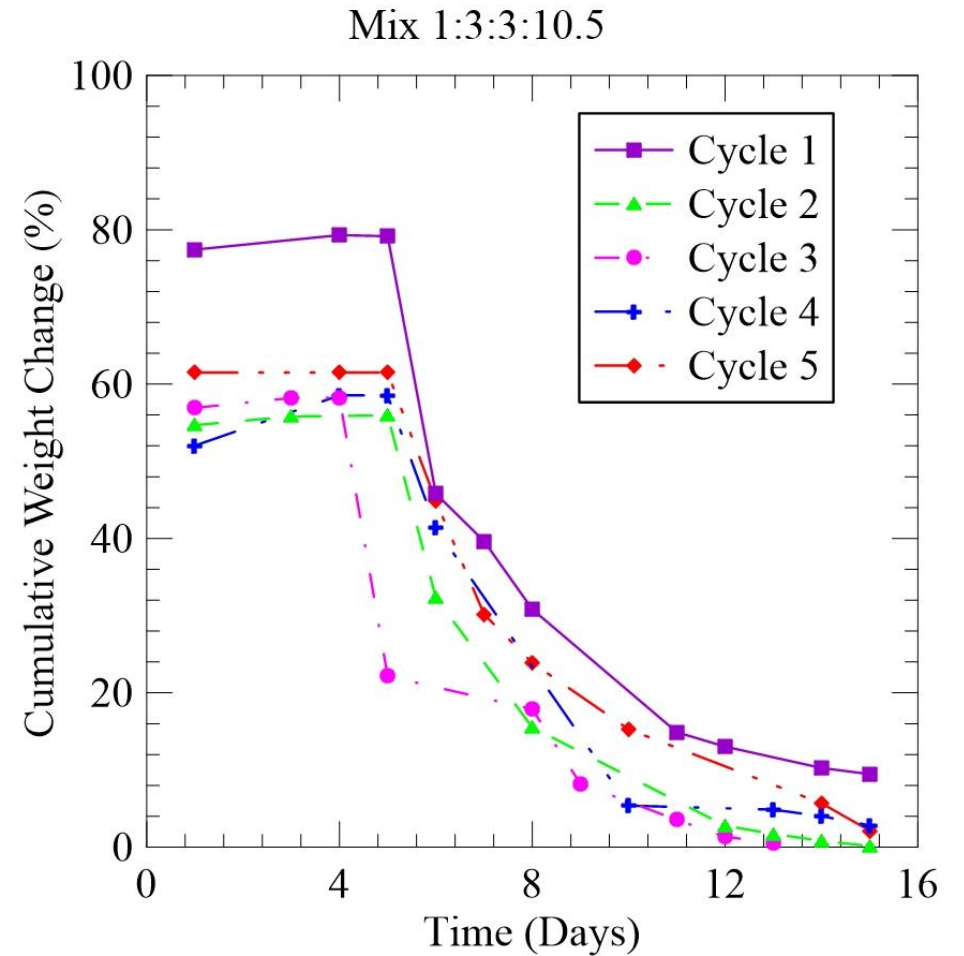
Split tensile strength samples



# Results - 4°C-20°C-50RH-SW



Weight change vs time for cycle 5

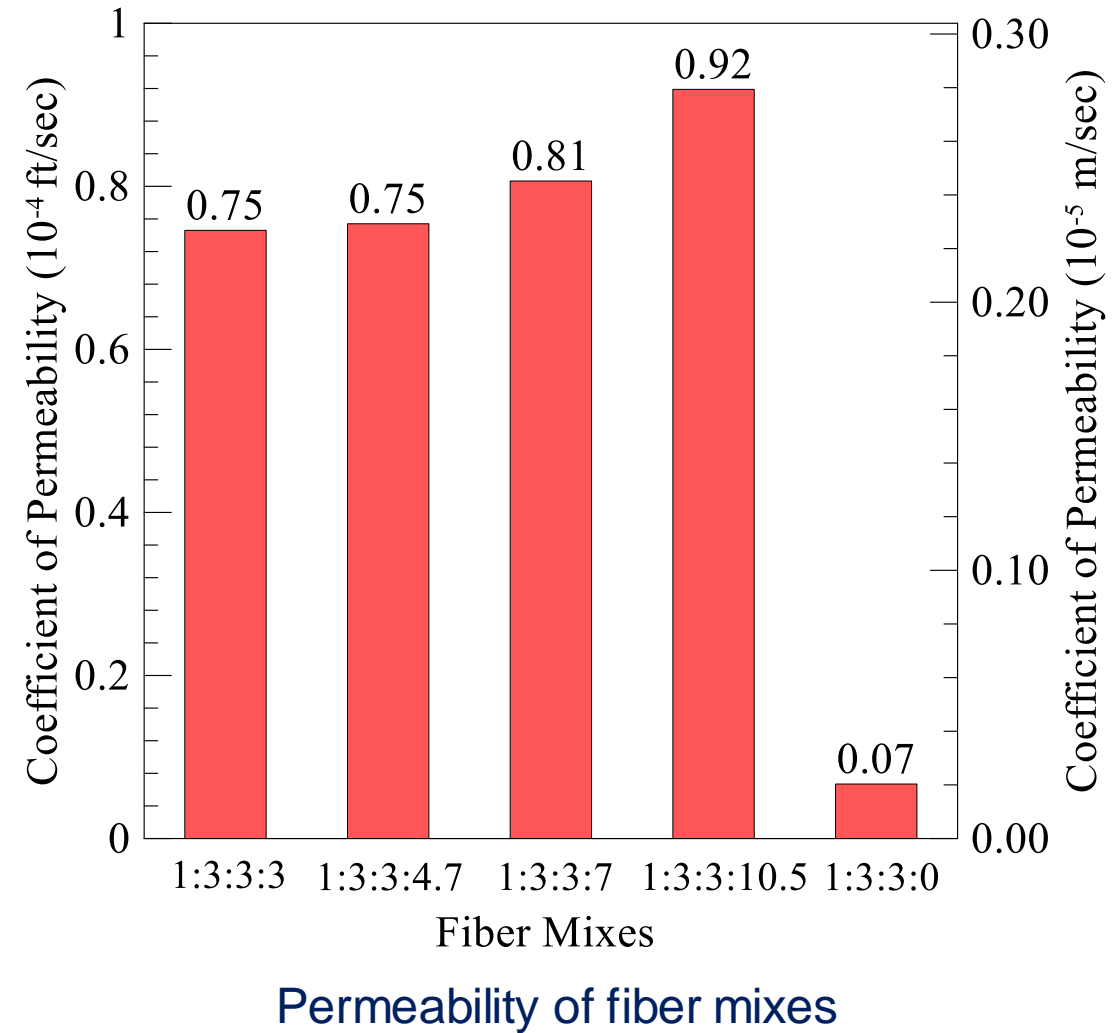


Weight change vs time for mix 1:3:3:10.5

- ❖ Fiber dosage  $\uparrow \rightarrow$  Weight change due wetting and drying  $\uparrow$
- ❖ Water absorption after 2 days is constant in all the fiber mixes

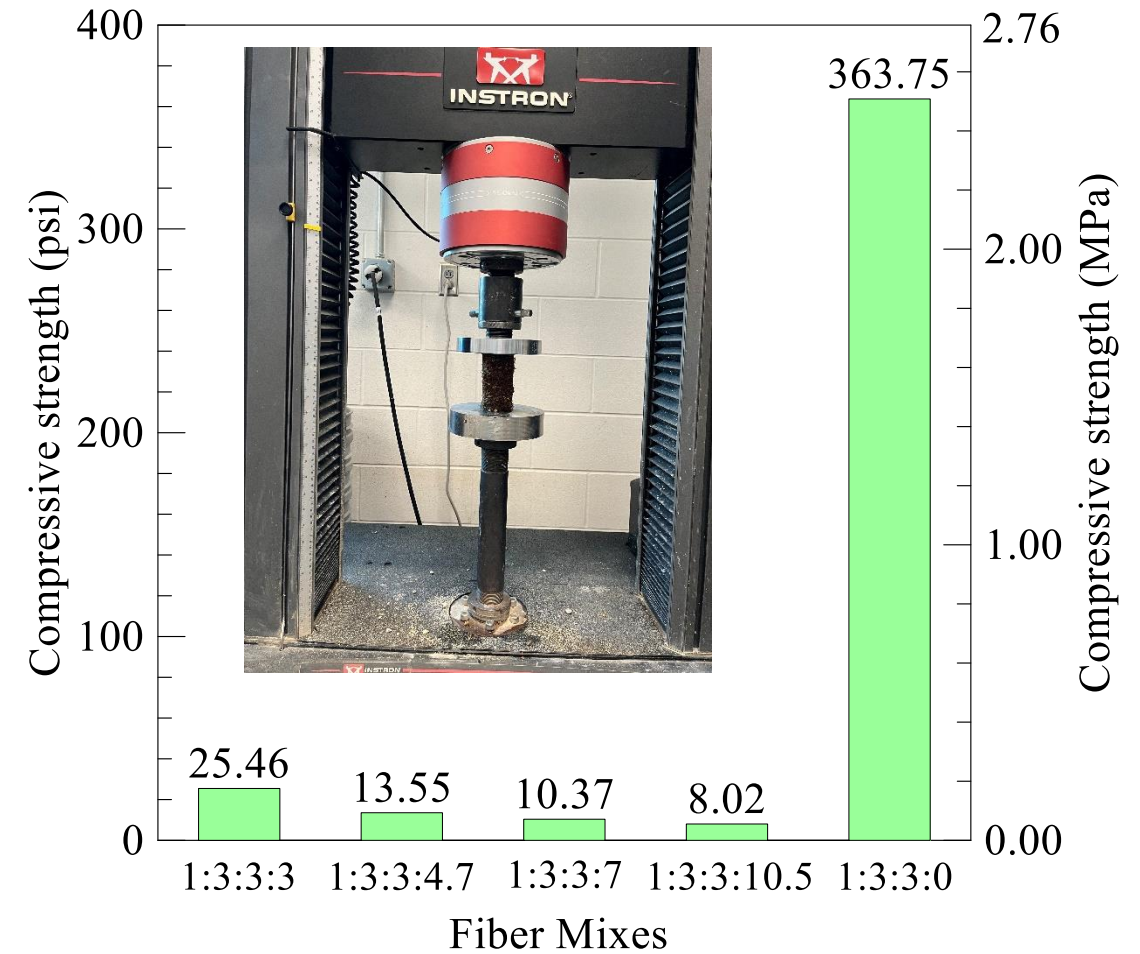
## Results – Permeability

- ❖ The coefficient of permeability,  $k$  of the fiber mixes was similar range of sand permeability (Das et.al 2017)
- ❖ The control mix showed the lowest permeability among the fiber mixes
- ❖ The permeability of control mixes is  $7 \times 10^{-6}$  ft/sec which fall in range of pervious concrete (Qin et.al 2015)



# Results – Compressive Strength

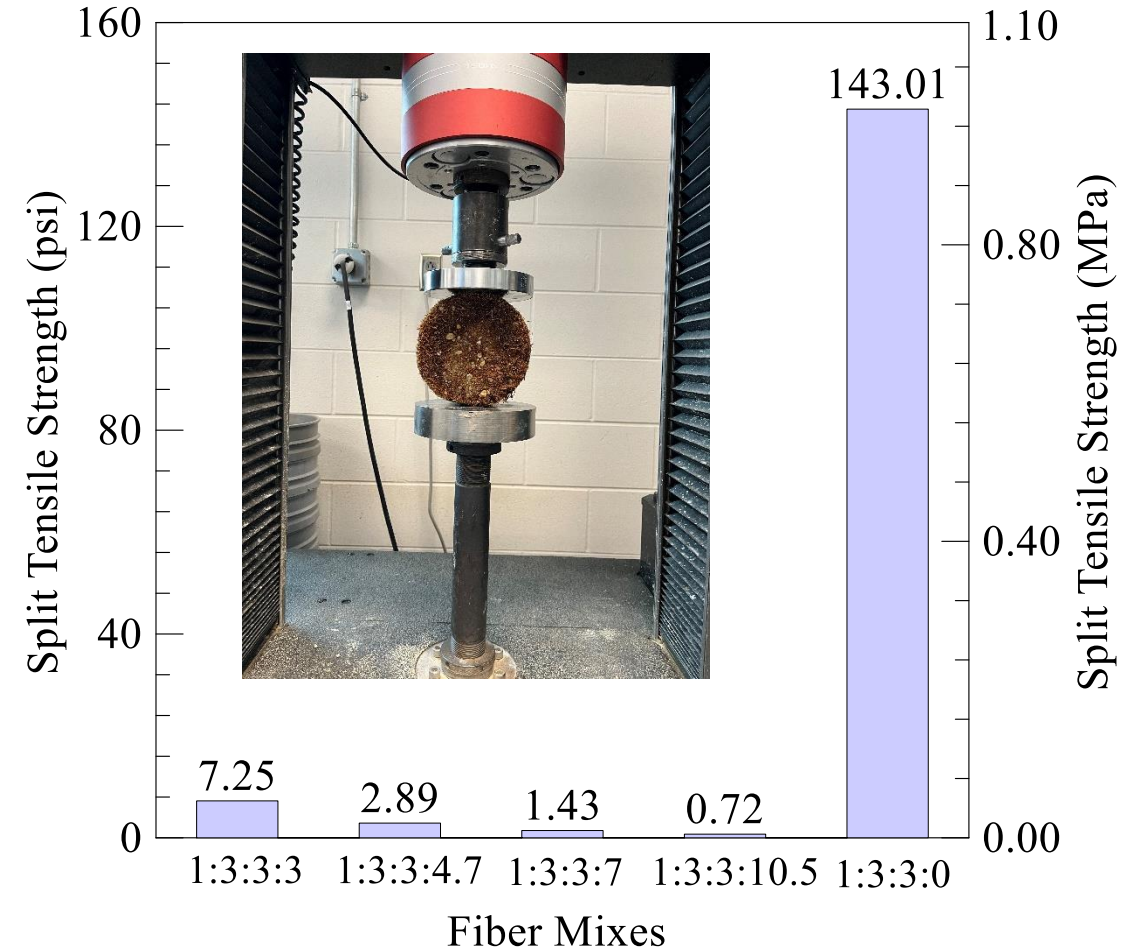
- ❖ Concrete mix has the highest compressive strength compared to other fiber mixes
- ❖ Compared to concrete control mix all fiber mixes showed elastic properties
- ❖ The fiber mixes showed very low compressive strength ranging from 25.46 psi to 8.02 psi corresponding to 10% strain.



Compressive strength of fiber mixes after 28 water curing

# Results – Split Tensile Strength

- ❖ Concrete mix has the highest split tensile strength compared to other fiber mixes
- ❖ All fiber mixes showed better elastic properties compared to the concrete control mix
- ❖ The fiber mixes showed very low tensile strength ranging from 7.25 psi to 0.72 psi



Split tensile strength of fiber mixes after 28 water curing

## Observations

- ❖ **Fiber mixes experienced higher water absorption and desorption (A & D) compared to control mixture**
  - ❑ **Control mix - 1:3:3:0 – Lowest A & D in all testing environments**
  - ❑ **Fiber mix - 1:3:3:10.5 – Highest A & D in all testing environments**
- ❖ **Percent fiber in mixes increases water absorption and desorption**
- ❖ **The coefficient of permeability of fiber mixes ranged between 7.5 to 9.2 x 10<sup>-5</sup> ft/sec**
- ❖ **Control mix has better strength properties compared to fiber mixes**

# Future Work

- ❖ Large scale laboratory testing

# References

- ❖ **ASTM Standard D2166, (2016) . "Standard Test Method for Unconfined Compressive Strength of Cohesive Soil," ASTM International, West Conshohocken, PA, DOI: 10.1520/D2166\_D2166M-16, [www.astm.org](http://www.astm.org)**
- ❖ **ASTM Standard D5084, (2016). "Standard Test Methods for Measurement of Hydraulic Conductivity of Saturated Porous Materials Using a Flexible Wall Permeameter," ASTM International, West Conshohocken, PA, DOI: 10.1520/D5084-16A, [www.astm.org](http://www.astm.org)**
- ❖ **Das, Braja M., Sobhan, K., (2017). Principles of Geotechnical Engineering (Ed. 9th). Massachusetts: Cengage Learning**
- ❖ **Qin Y., Yang H., Deng Z., He J., (2015). "Water Permeability of Pervious Concrete Is Dependent on the Applied Pressure and Testing Methods", Advances in Materials Science and Engineering, 2015 (404136). <https://doi.org/10.1155/2015/404136>**

# LIFE FORMS

**Project: Evaluating the Performance of Fiber-Based Concrete Mixes for Various Applications**

**Number: 5**





# Application of Geof foam in Thermal Encapsulation of Foundations

**Project Leader:** Hiramani R. Chimaurya

**Team:** Clay Caldwell, Nripojyoti Biswas, Surya S C  
Congress

**PI:** Anand J. Puppala

Professor | A.P. and Florence Wiley Chair  
Director – Center for Infrastructure Renewal

Closed Meeting

TAMU Site Proprietary

NSF IUCRC CICI TAMU SITE  
NSF IUCRC CICI - IAB Spring 2023 Meeting

May 8-9, 2023



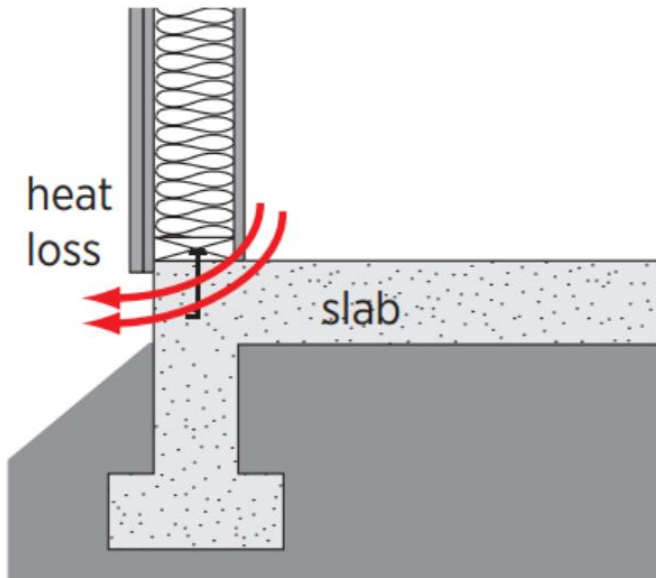
# Presentation Outline

- ❑ Introduction
- ❑ Test Methodology
- ❑ Control Test (Baseline)
- ❑ Geofam Around Footing (GAF) Tests
  - GAF 8-in. Test
  - Indoor Temperature: Control vs GAF
- ❑ Results Summary
- ❑ Conclusions
- ❑ Future Work



# Introduction

- ❑ Temperature fluctuations inside the dwellings typically occur from advection, diffusion and radiation at foundation superstructure joints
- ❑ About 15% of all heat loss in a home is through floors or basements
- ❑ Thermal Encapsulation using Geofoam
  - Research Plan
  - Laboratory Testing Setups

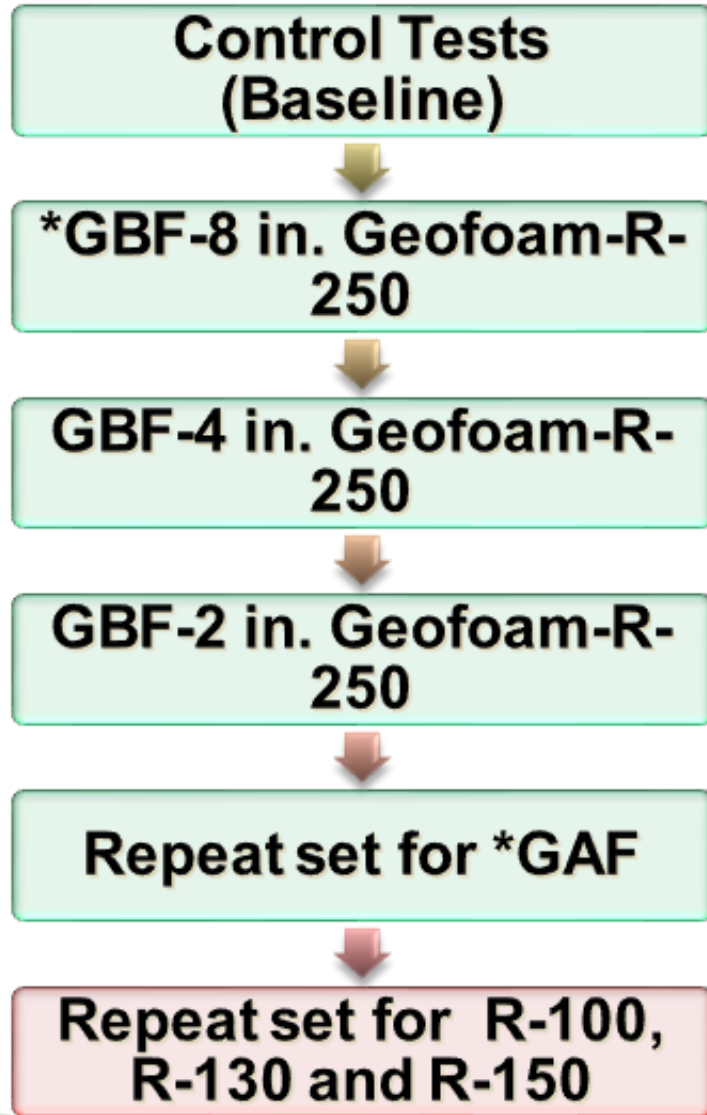


Heat loss



The stack effect

# Test Methodology



COMSOL  
Modeling of  
Laboratory Tests

Initial  
Setup



Final Setup



\*GBF: Geofam Below Foundation  
GAF: Geofam Around Foundation

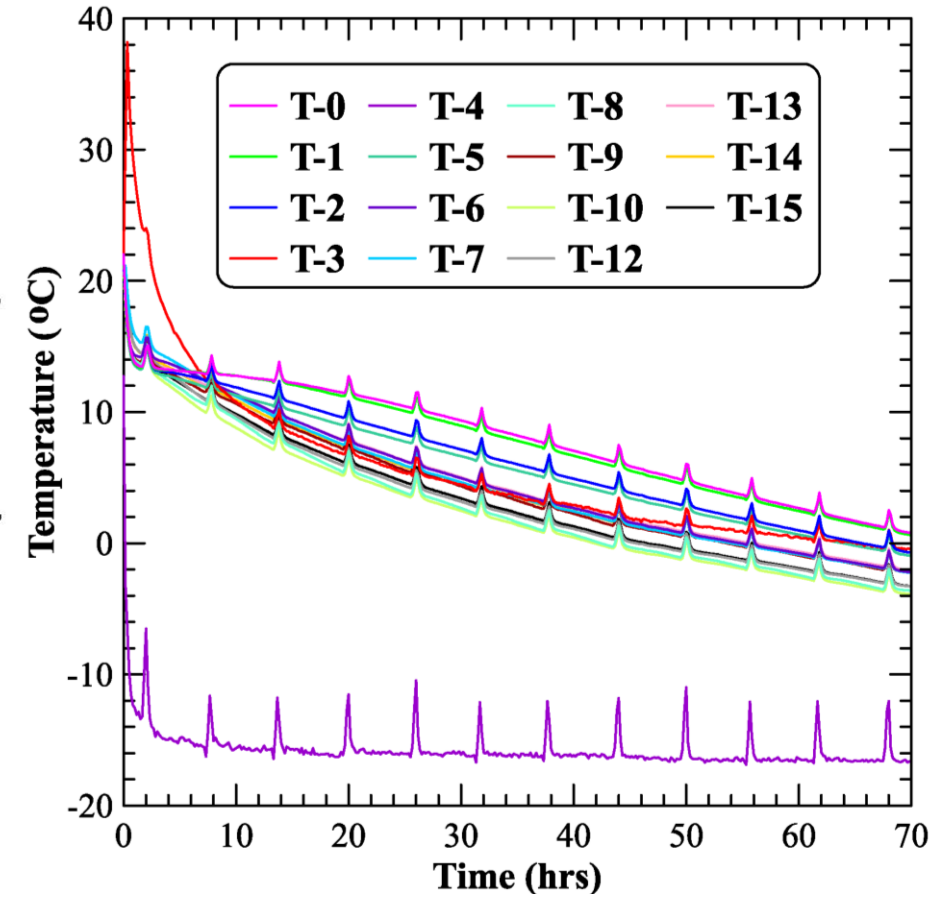
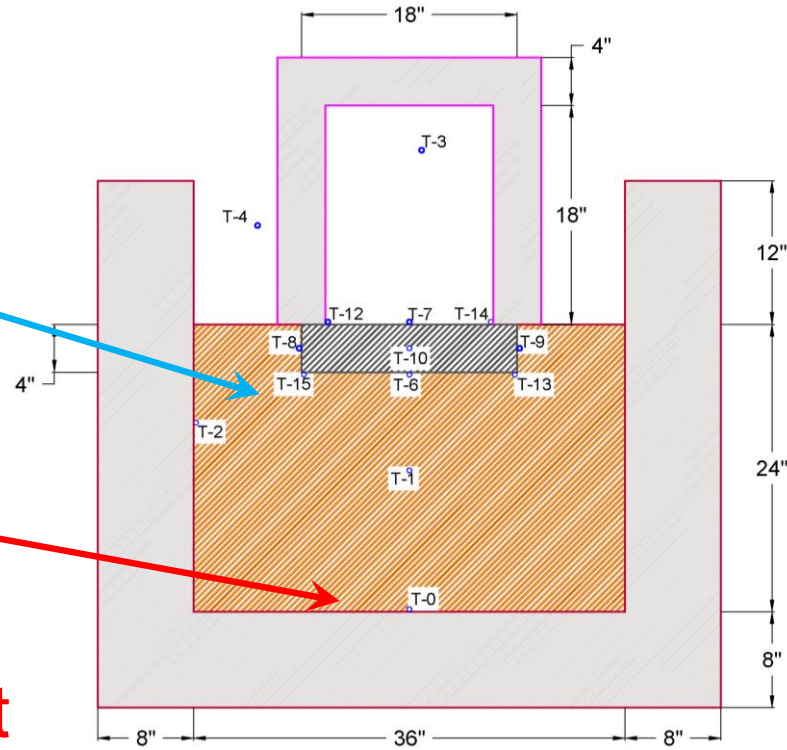


TEXAS A&M UNIVERSITY

Zachry Department of Civil &  
Environmental Engineering

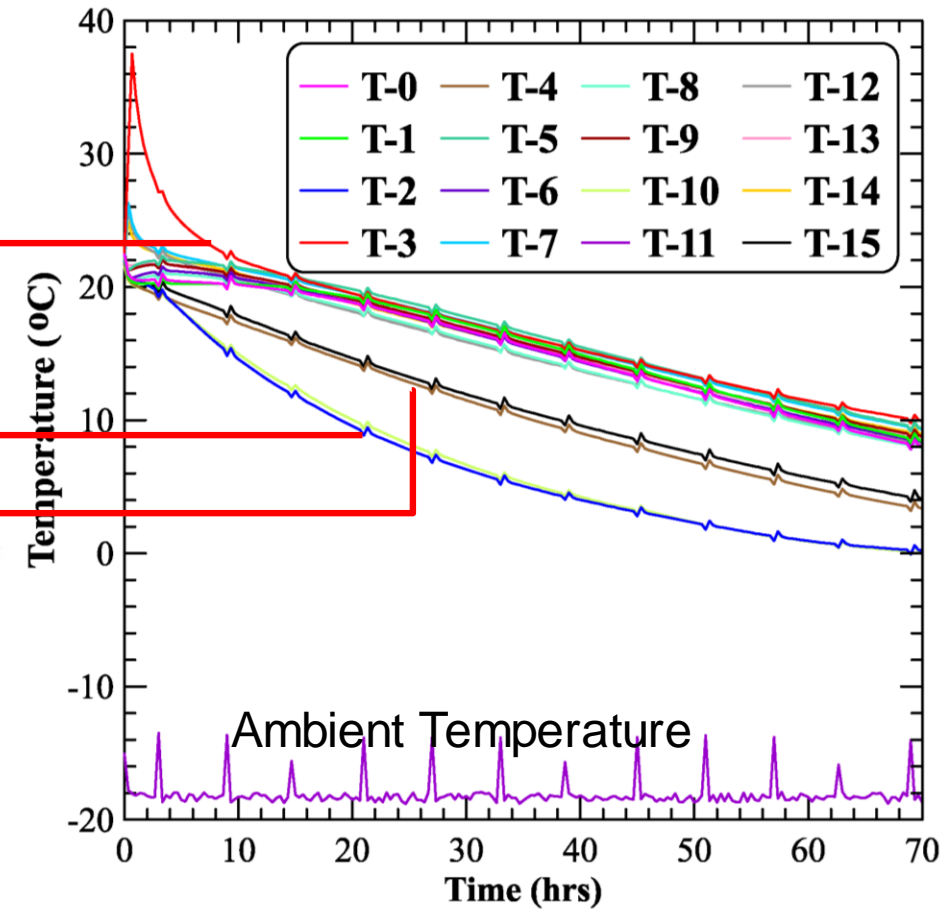
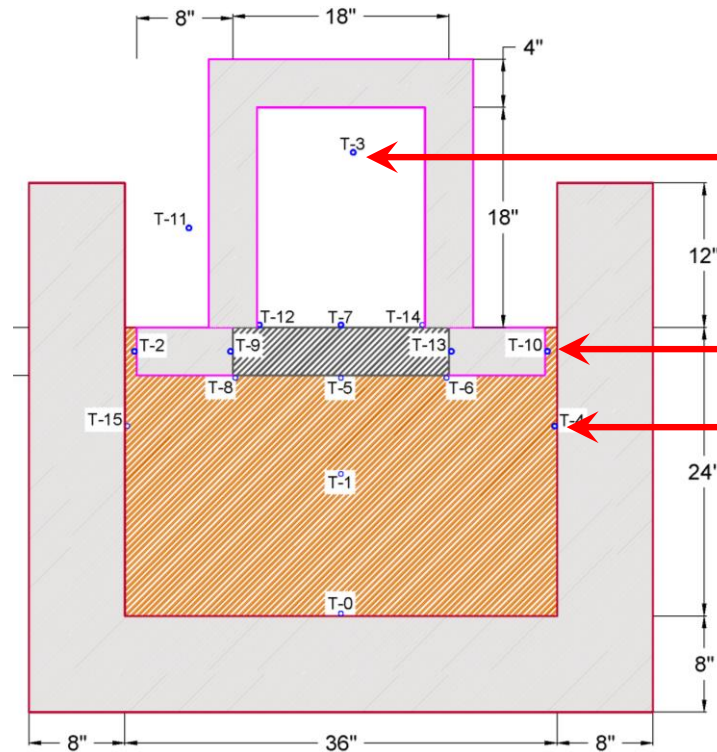
# Control Test (Baseline)

- ❑ “Bands” of temperature zones
- ❑ Slab-soil interface locations – **coldest**
- ❑ Bottom of the test box – **warmest**
- ❑ Indoor over  $2^{\circ}\text{C}$  warmer – **loss of heat to soil** is cooling the slab



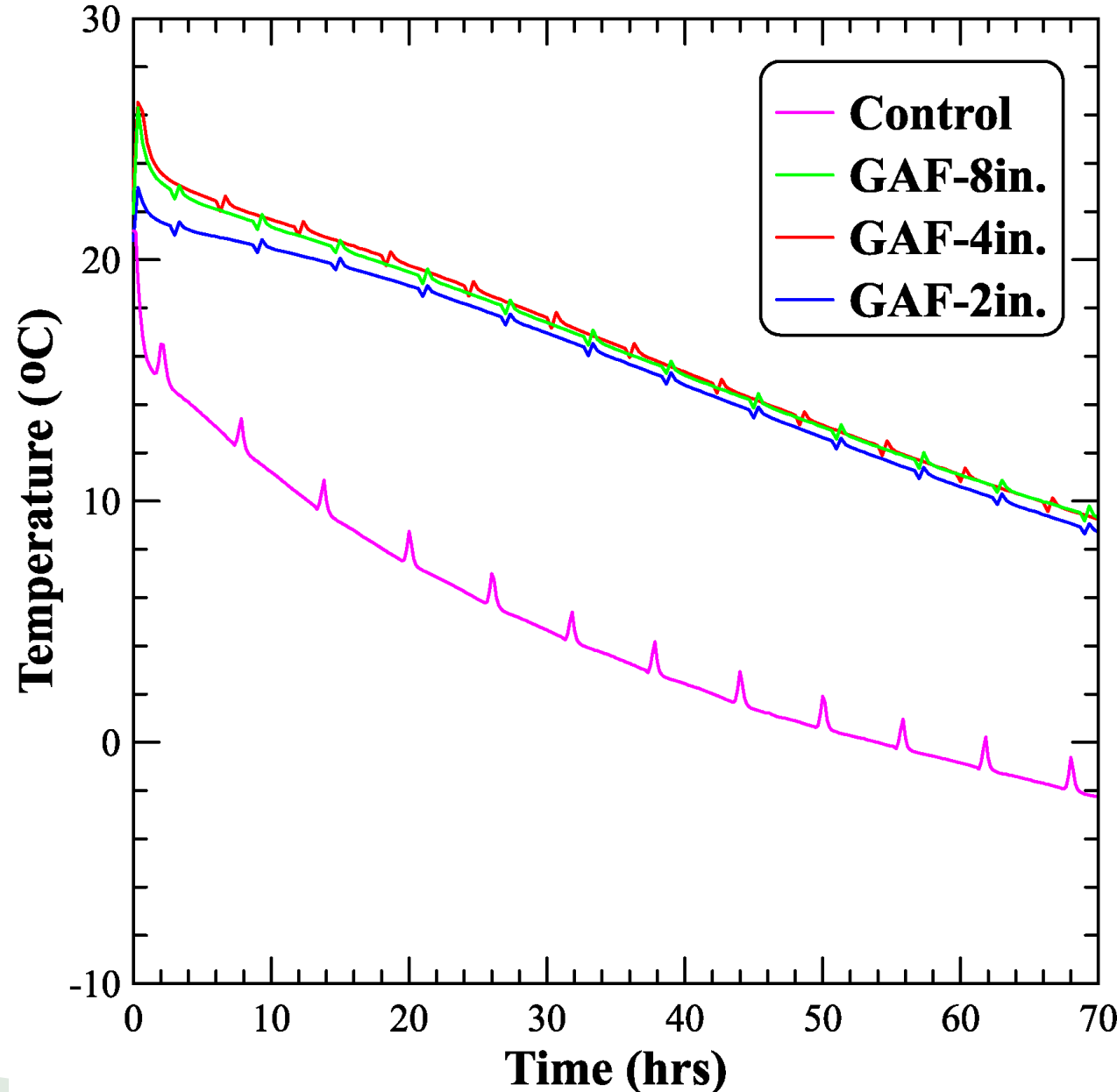
# GAF 8-in. Test

- ❑ Temperature fluctuations between locations significantly reduced
- ❑ Significantly warmer indoor temperature compared to control test ( $>10^{\circ}\text{C}$ ) warmer
- ❑ Increased temperature observed within the whole setup – reduced heat loss
- ❑ Side walls – coldest



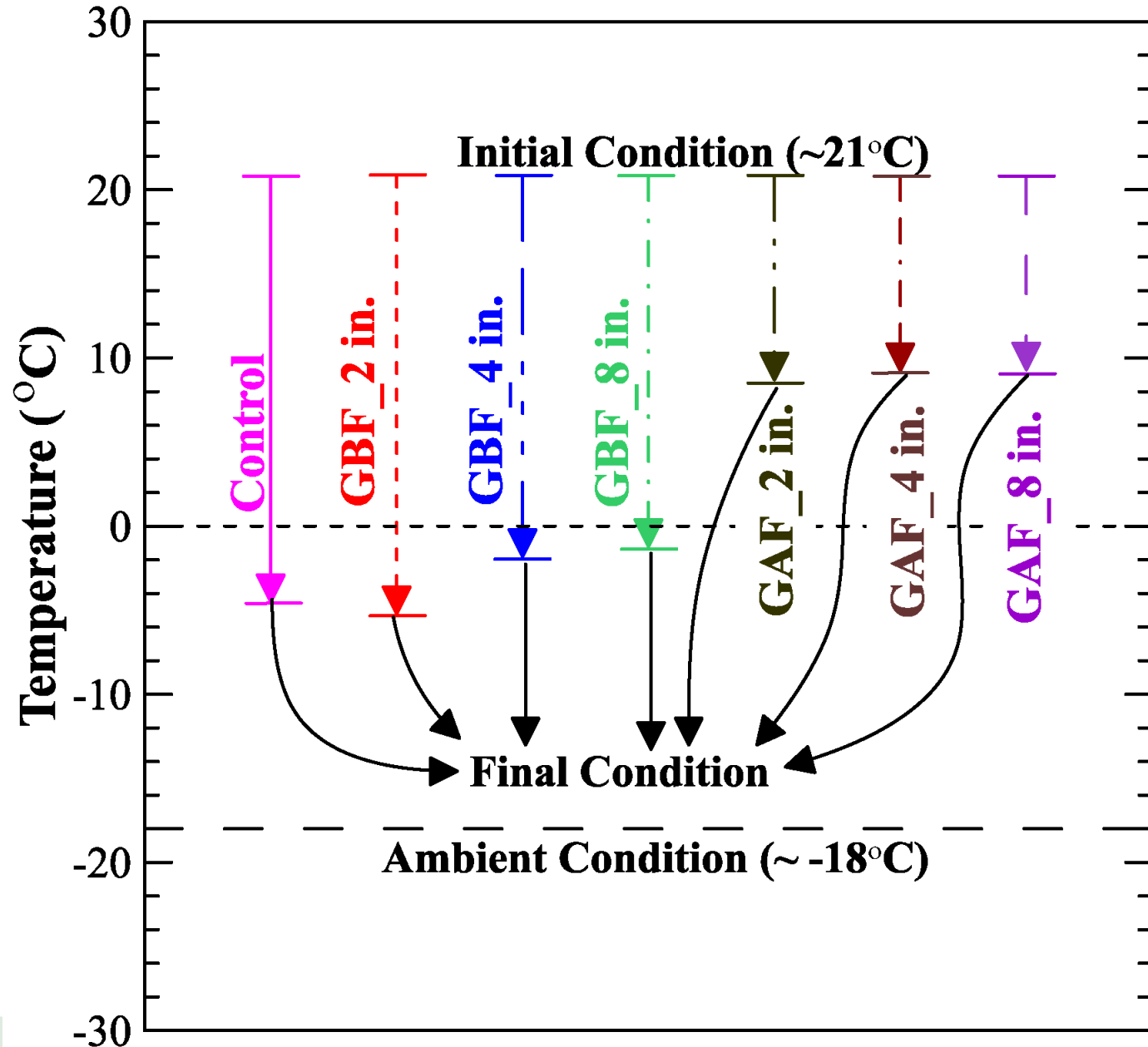
# Indoor Temperature: Control vs GAF

- ❑ Similar trend of increased temperature observed in all 3 GAF tests.
- ❑ While significant increase in performance was observed compared to control test, not much difference was observed between different thicknesses
- ❑ Comparing the gain in performance, the 2 in. thick geofoam might be more efficient than 4 in. and 8 in. options



# Results Summary

- ❑ GAF configurations significantly outperform all GBF tests
- ❑ GAF sections had  $>8^{\circ}\text{C}$  warmer indoor temperature than GBF sections and  $>10^{\circ}\text{C}$  warmer than Control section
- ❑ Not much difference in performance for thicker insulation  $\rightarrow$  2 in. GAF more efficient





# Conclusions

- ❑ Two configurations of geof foam insulation on slab-on-grade foundation tested
- ❑ Two modes of heat transfer influenced by the tested configurations:
  - Heat lost to the soil below the footing (GBF)
  - Heat lost to ambient air through shallow soil layer (GAF)
- ❑ Better performance of GAF → Heat lost to ambient air controlling factor
- ❑ Thickness of geof foam has less influence than the insulation configuration
- ❑ 2 in. thick geof foam, under GAF configuration found to be most suitable option

# Future Works

- ❑ Repeat lab tests for other grades of geofoam
- ❑ Numerical Simulation of GBF and GAF Tests

## OUTCOMES

- ❑ Clay Caldwell is recruited as a PhD student
- ❑ We submitted ASCE Geocongress paper – Geotechnical Special Publication

# LIFE FORMS

**Project:** Application of Geofom in Thermal Encapsulation of Foundations

**Number:** 6



# Design and Testing of IFI Geosynthetic Products

**Project Leader:** Md Ashrafuzzaman Khan

**Team Members:** Krishneswar Ramineni  
Clay Caldwell, Nripojyoti Biswas

**PI:** Anand J. Puppala

Professor | A.P. and Florence Wiley Chair  
Director – Center for Infrastructure Renewal

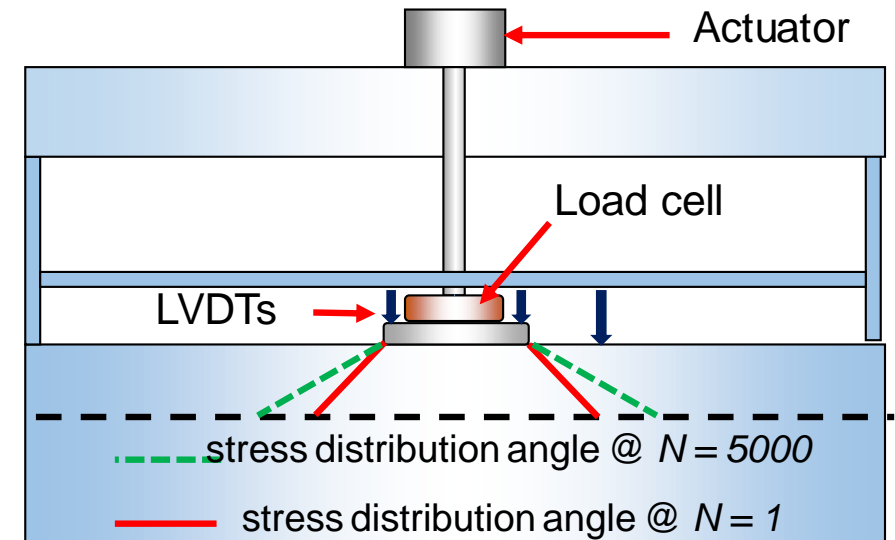
Closed Meeting

TAMU Site Proprietary

NSF IUCRC CICI TAMU SITE  
NSF IUCRC CICI - IAB Spring 2023 Meeting

# Outline of the Presentation

- ❑ Background and Objective
- ❑ Laboratory Investigation
- ❑ Results
- ❑ Model Calibration
- ❑ Design Procedure
- ❑ Summary



Large-scale Testing Set up (6' x 6' x 2.5')

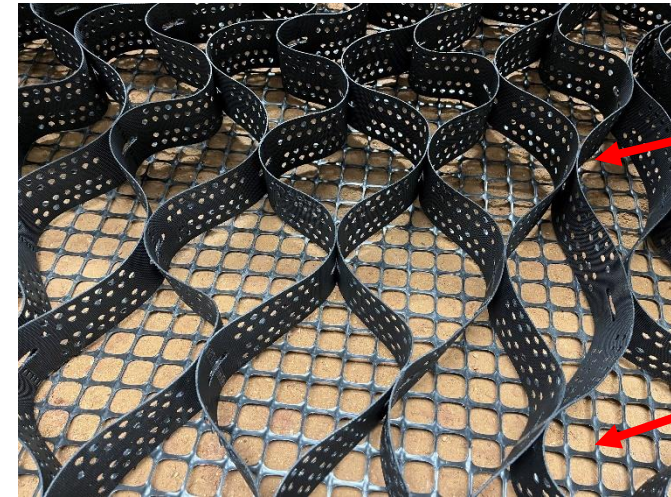
# Background and Objective

## Background:

- ❑ Need to evaluate the effectiveness of different IFI products based on laboratory testing
- ❑ Need to calibrate the design equation
- ❑ Need to develop design charts to assist the engineer for future design

## Objective:

- ❑ Perform large-scale repeated load test to quantify the benefits from different IFI products
- ❑ Develop design charts and tables for unpaved and paved roads with geosynthetics



3D Geocell

2D Geogrid

Product ID	Product Type	Aperture stability m-N/deg.	Height (in.)
BL5	Planar	0.80	-
BL6	Planar	0.98	-
BL7	Planar	1.50	-
FG6 (FAB)	Planar	0.98	-
GG4	3D	-	4
GG6	3D	-	6

# Laboratory Investigation Testing Plan

**Table : Large-Scale Cyclic Plate Load Testing Plan**  
**Note: UR- Unreinforced; GG- Geogrid; GC- Geocell; FG- Fabgrid**

Testing Sequence	Test Designation	Geosynthetic type	Subgrade Soil: CBR value	Number of tests as per plan	Remarks
1	Unreinforced (Control)	-	1 & 3	2	Completed (4 additional)
2a	FG	Fabgrid (FG6)	1 & 3	2	Completed
2b	GG	Geogrid (BL5, BL6, BL7)	1 & 3	6	Completed
3a	GC	Geocell (4 in.)	1 & 3	2	CBR=1 completed, CBR = 3 completed
3b	GC	Geocell (6 in.)	1 & 3	2	CBR=1 completed, CBR = 3 completed
4a	GG:GC	Geocell (4 in.) + BL6	1 & 3	2	CBR=1 completed, CBR = 3 completed
4b	GG:GC	Geocell (6 in.) + BL6	1 & 3	2	CBR=1 completed, CBR = 3 completed
<b>Total number of testing:</b>				18	

# Laboratory Investigation

## Design parameters

❑ Reinforcement were placed at the interface of base and subgrade layer

❑ Main objective of the repeated load testing was to determine the load distribution angles with the number of loading cycles

$$h = \frac{r}{\tan \alpha} \left( \sqrt{\frac{P}{\pi r^2 p_i}} - 1 \right)$$

$p_i$  = normal stress at the interface of base and subgrade layer (kPa)

$P$  = wheel load (KN)

$r$  = radius of the equivalent tire contact area (m)

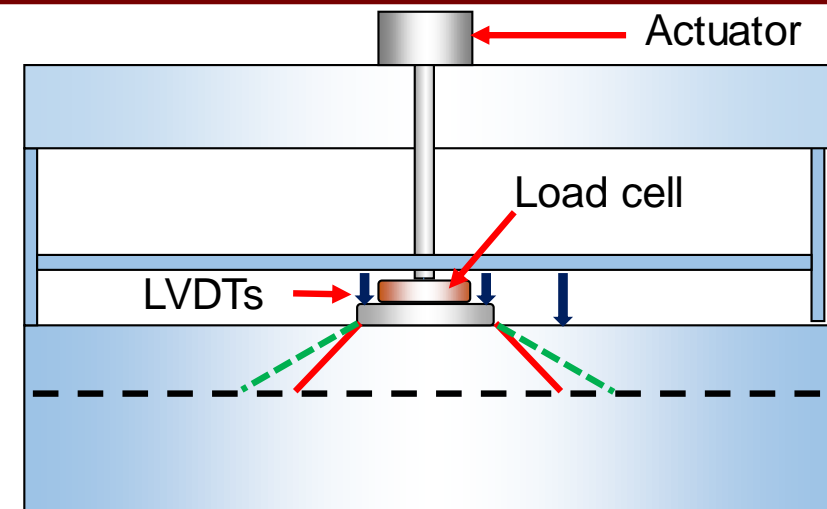
$h$  = thickness of the base layer (m)

$\alpha$  = stress distribution angle

$$\frac{1}{\tan \alpha} = \frac{1}{\tan \alpha_1} + \lambda^* \log N$$

$\alpha$  = stress distribution angle for the case where the number of passes is  $N$ ;

$\alpha_1$  = stress distribution angle for the case where the number of passes is one



--- stress distribution angle,  $\alpha$

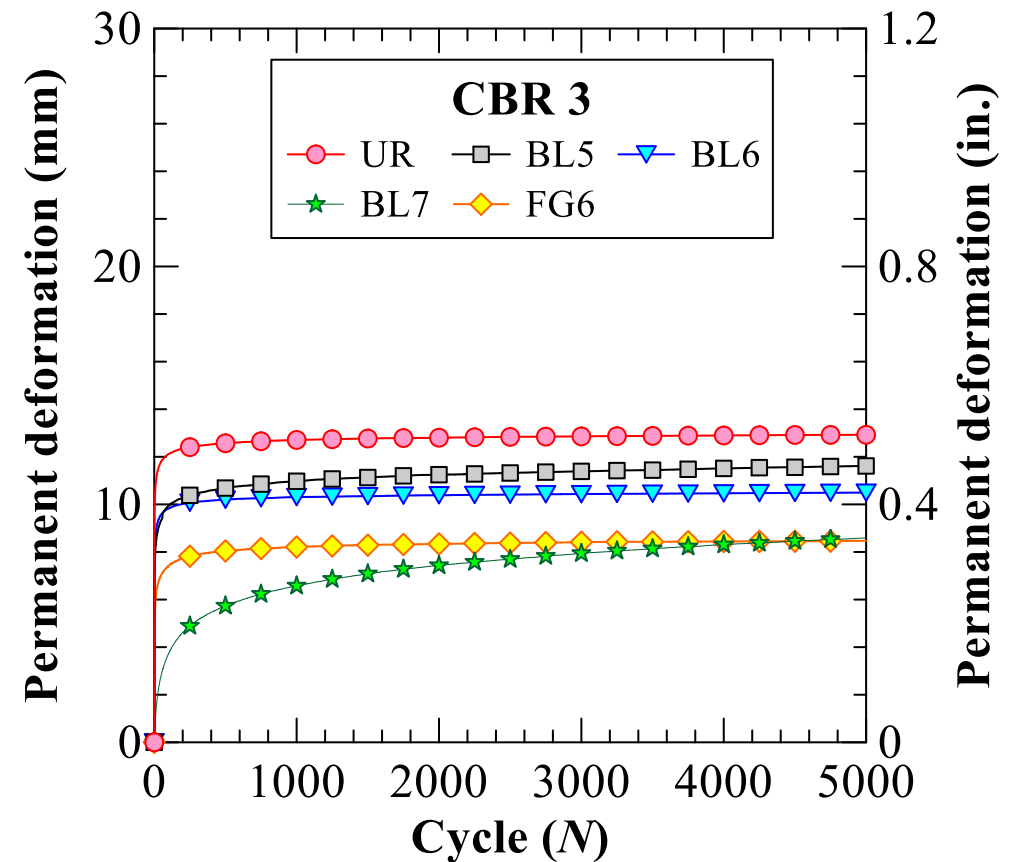
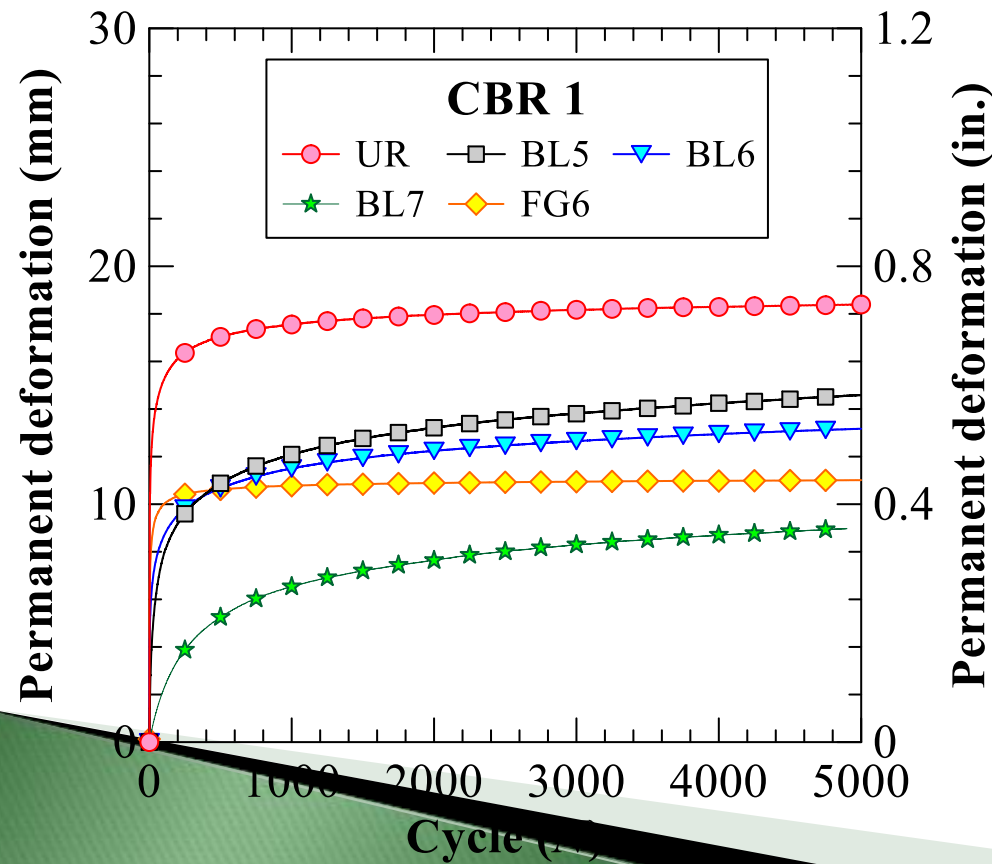
— stress distribution angle,  $\alpha_1$



# Results

## Planar Reinforcement (Geogrids)

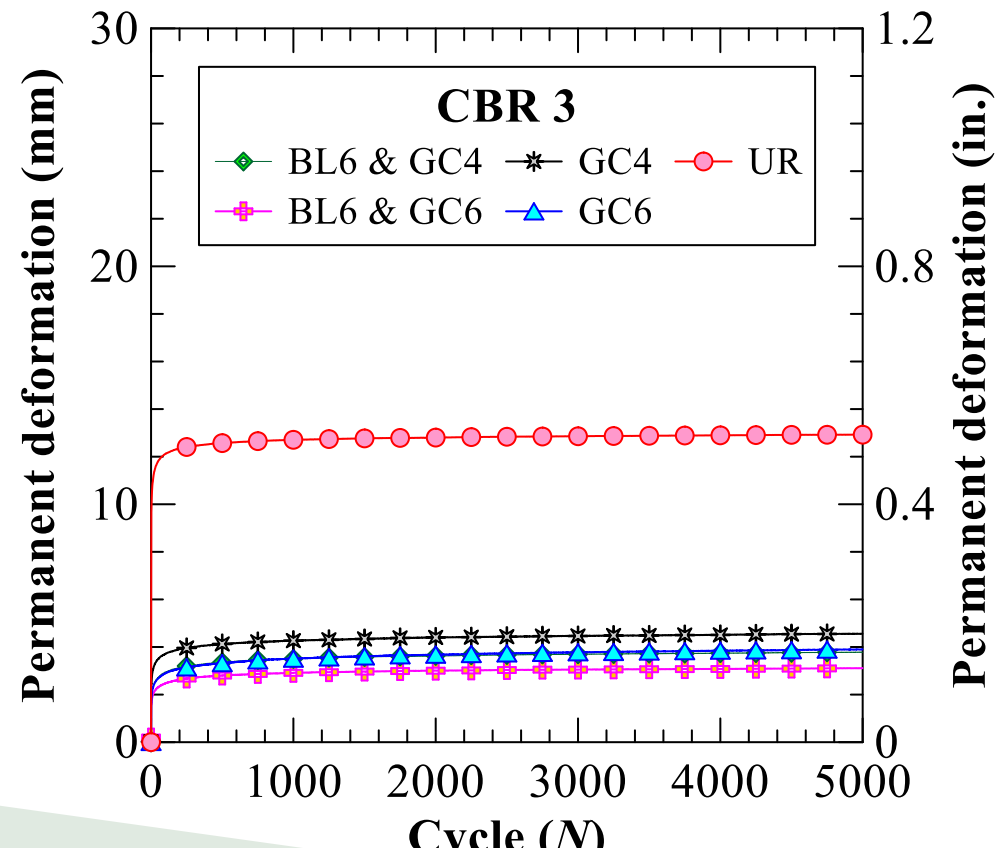
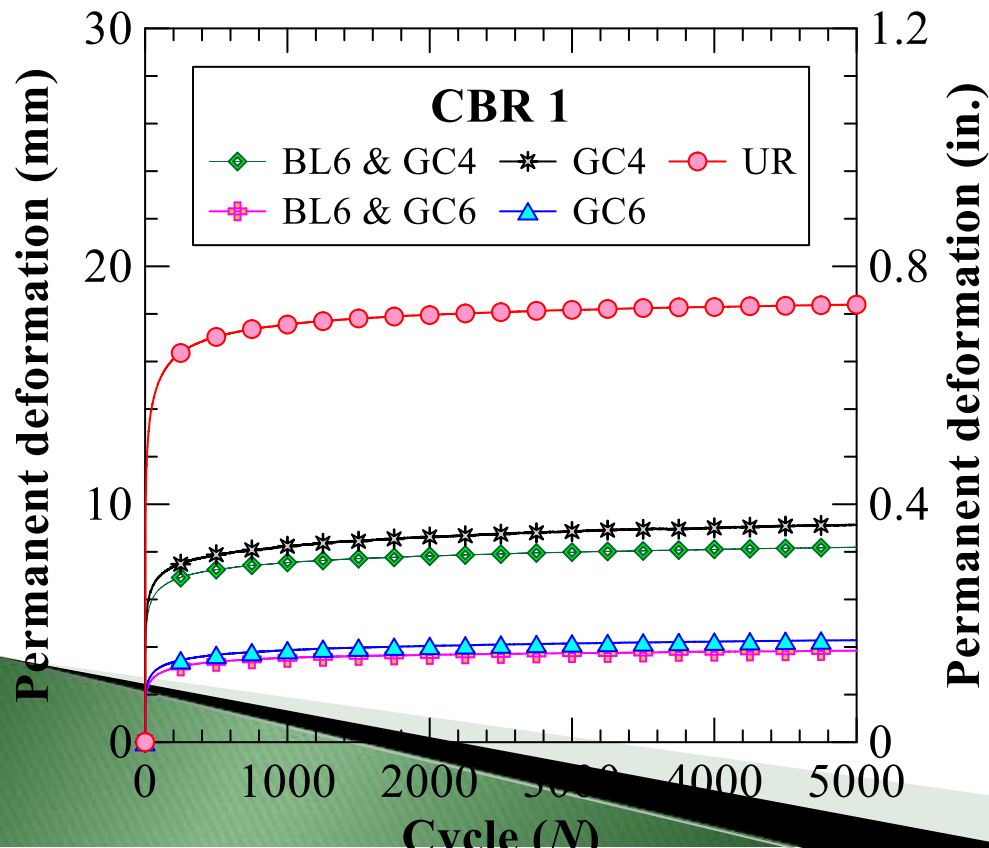
- Aperture stability modulus of geogrids:  $BL5 < BL6 < FG6 < BL7$
- Maximum permanent deformation (PD) after 5000 cycles:  $BL5 > BL6 > FG6 > BL7$
- PD for CBR 3  $\approx$  60 to 70% of CBR 1



# Results

## Effect of 3D Geosynthetic (Geocell)

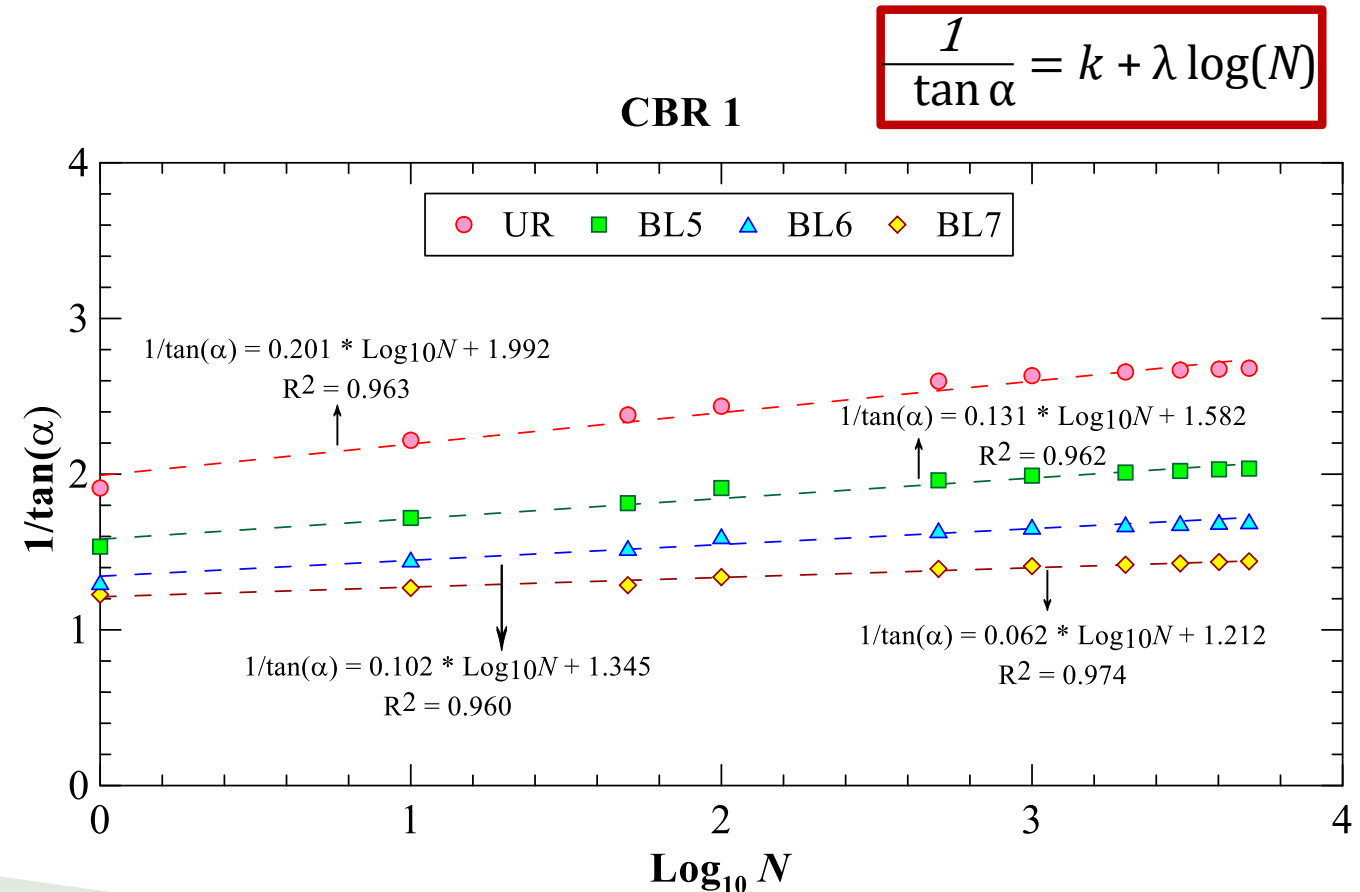
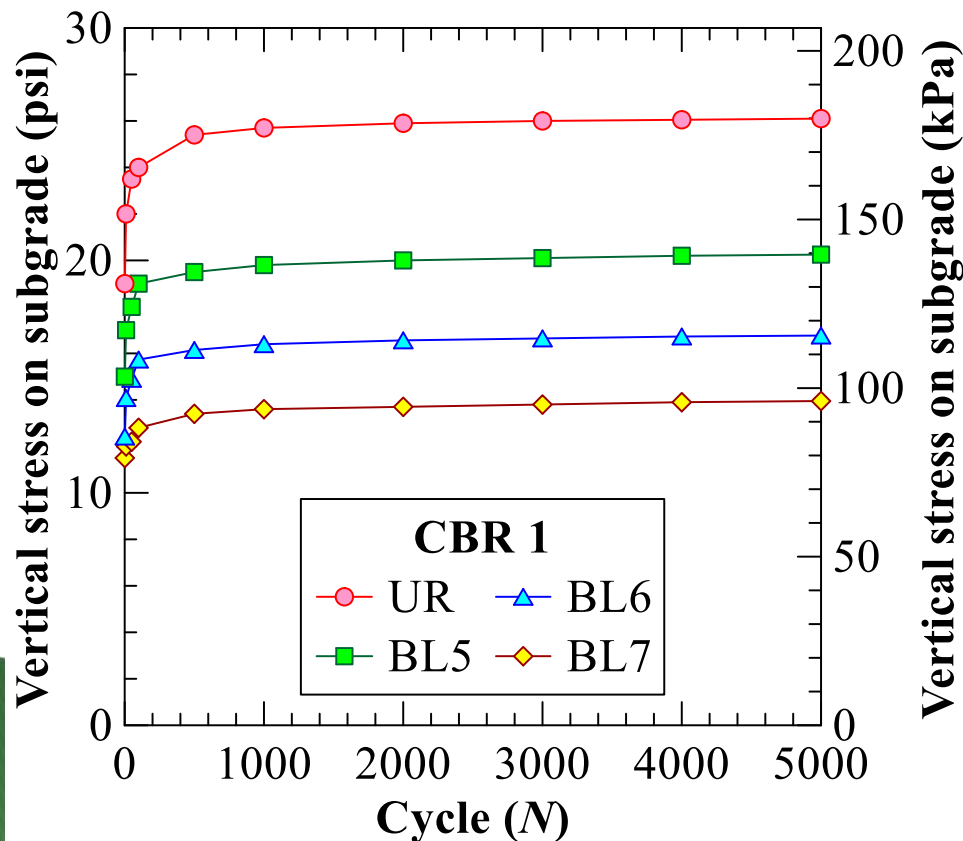
- Permanent deformation (PD) with Geocell → reduction **up to 4 times**
- 3D Geocell vs 2D geogrids → **2.6 times reduction**
- PD of (3D Geocell + 2D geogrids) vs 3D Geocell → **5-10 % reduction**



# Results

## Stress Distribution Angle for CBR = 1

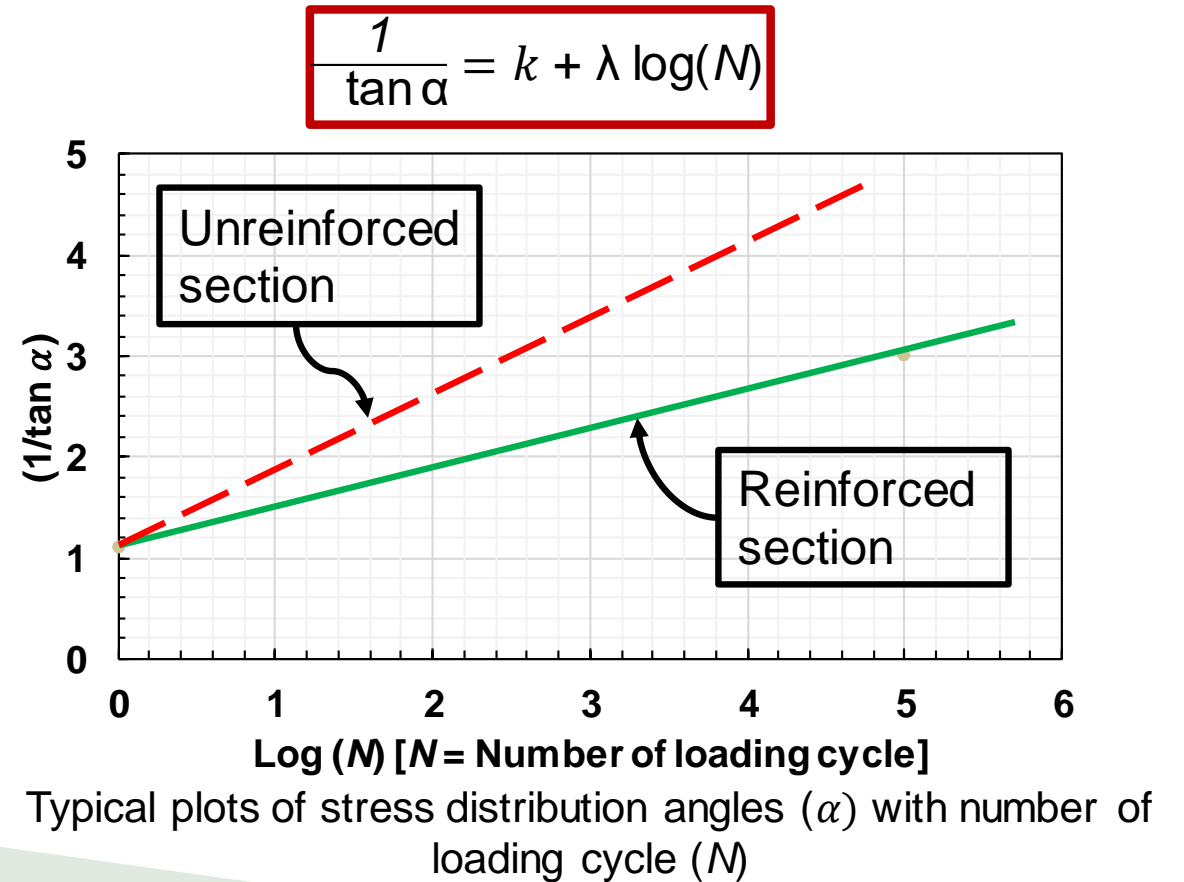
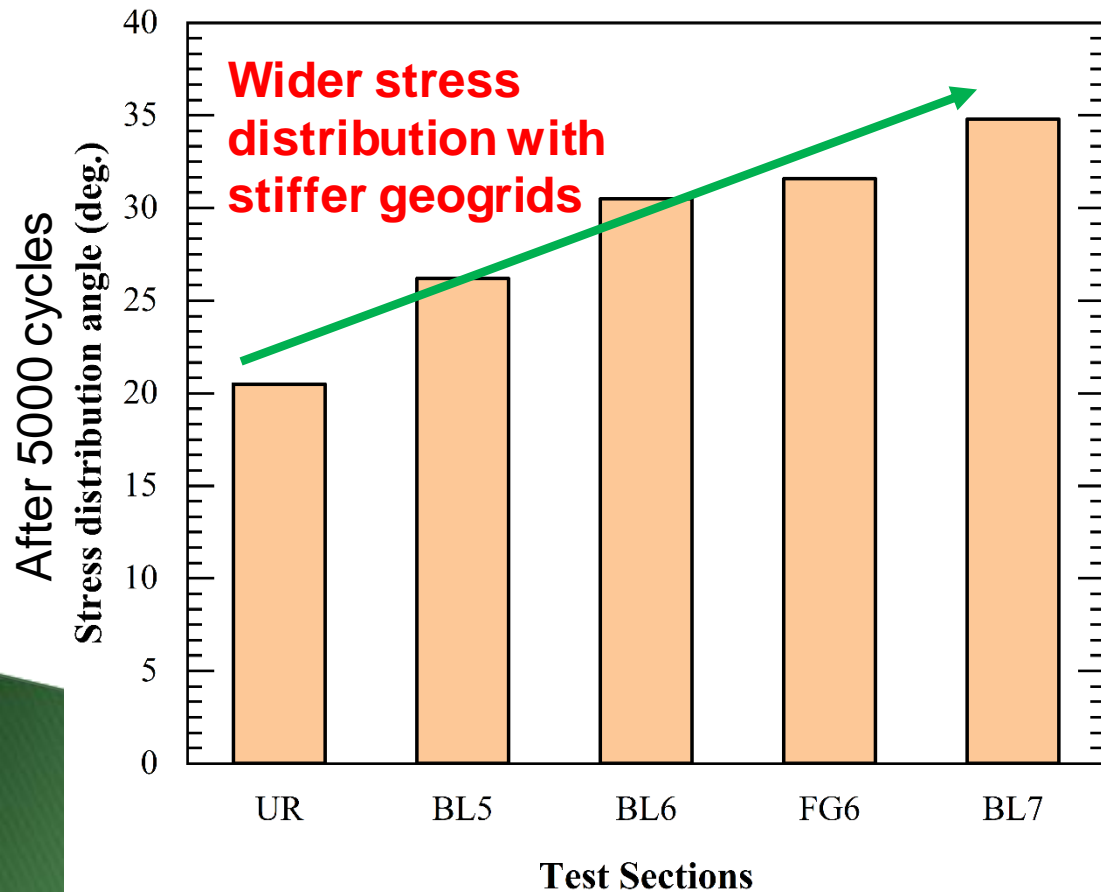
- Vertical stress on subgrade reduced with geosynthetic reinforcement
- Maximum vertical stress after 5000 cycles: BL5 > BL6 > BL7
- Vertical stress values were used to determine stress distribution angles



# Results

## Updated Design Parameters (geogrids only)

- ❑ Stress distribution angle ( $\alpha$ ) showed the improvement with geogrids
- ❑  $\alpha$  decreases with the number of loading cycles
- ❑ New calibration equation is under development including  $\lambda$  and  $k$  functions



# Model Calibration

## Updating $k$ & $\lambda$

S.N.	$E_2$ or $E_{subg}$	$E_1/E_2$ or $E_{base}/E_{subgrade}$	$r/h$	$j$	Remarks
1	5	4	1.0	0.00	G-H
2	5	4	1.0	0.32	G-H
3	5	4	1.0	0.65	G-H
4	5	4	0.6	0.00	G-H
5	5	4	0.6	0.32	G-H
6	5	4	0.6	0.65	G-H
7	1	5	0.5	0.00	Current
8	1	7	0.5	0.80	Current
9	1	11	0.5	0.98	Current
10	1	7	0.5	1.50	Current
11	3	3	0.5	0.00	Current
12	3	3.5	0.5	0.80	Current
13	3	5	0.5	0.98	Current
14	3	4	0.5	1.50	Current

$k$  &  $\lambda$

$$k = (0.62 - 0.41j + 0.13j^2)(E_1/E_2)^{0.59}(r/h)^{-0.11}$$

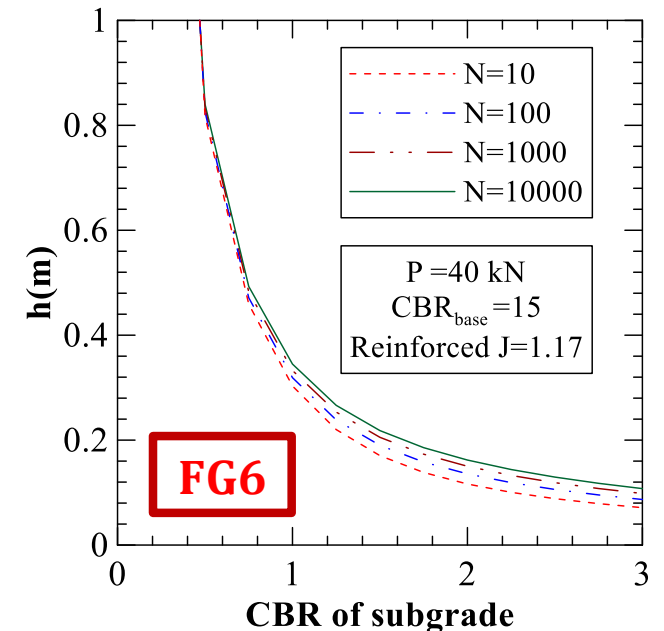
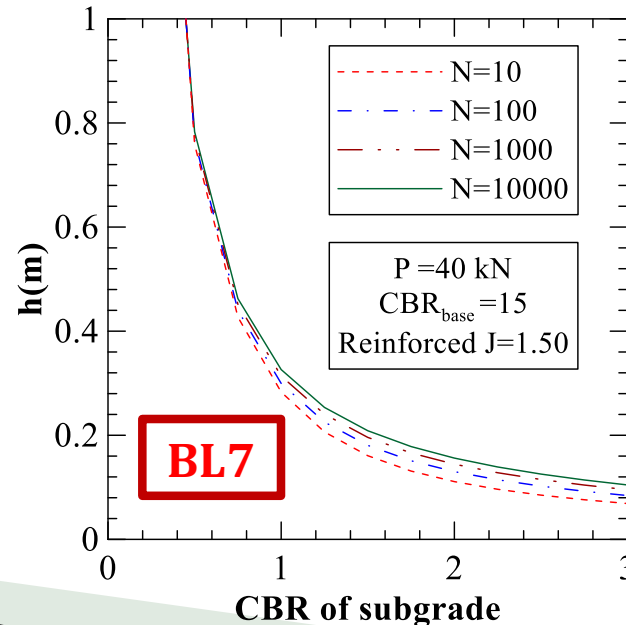
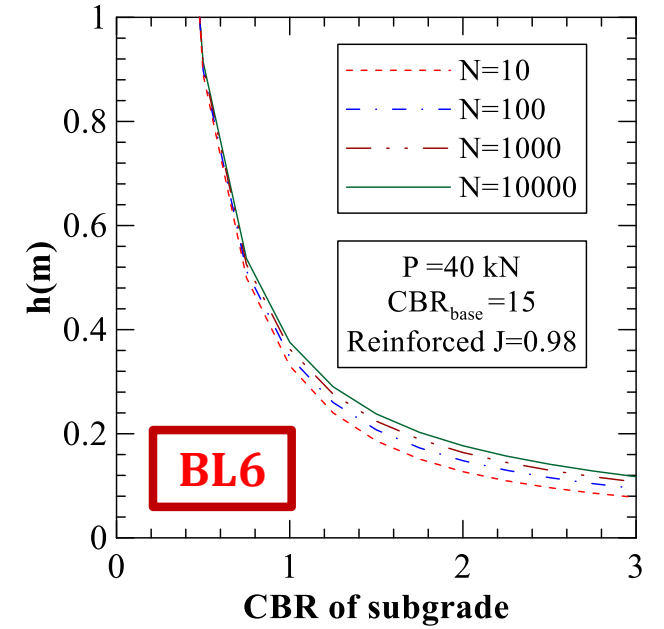
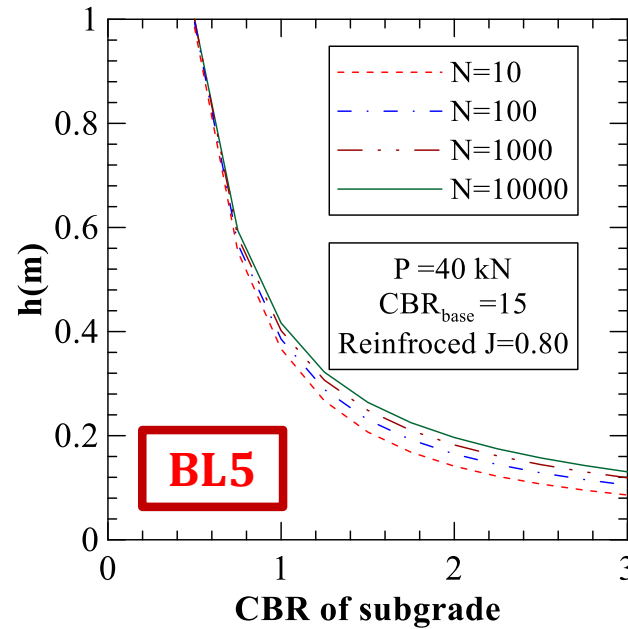
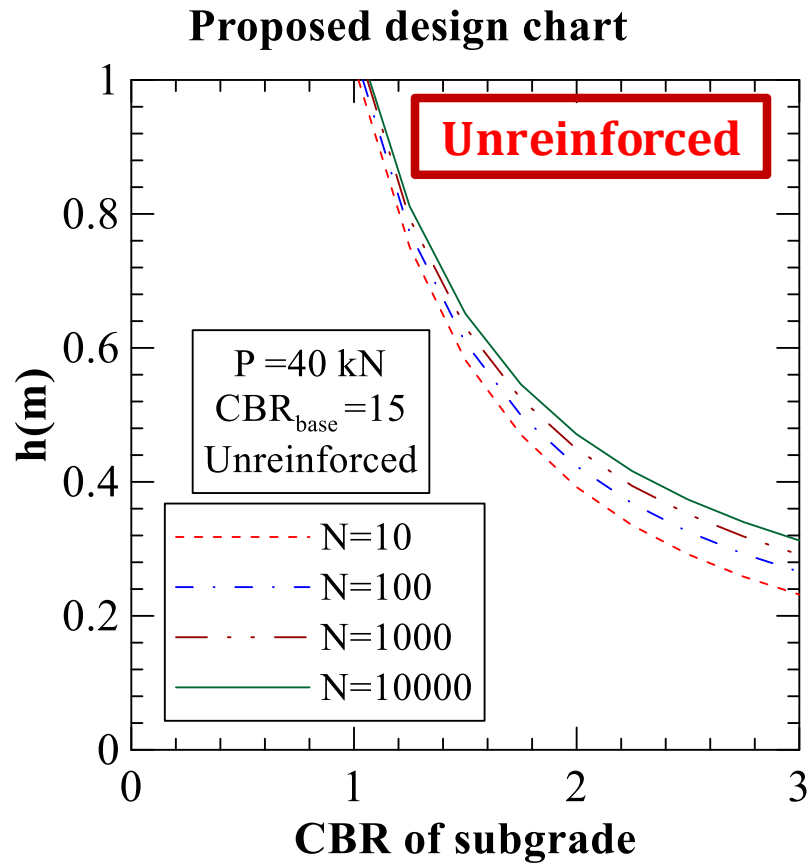
$$\lambda = (0.43 - 0.52j + 0.19j^2)(E_1/E_2)^{0.5}(r/h)^{1.74}$$

$$\frac{1}{\tan \alpha} = k + \lambda \log(N)$$

$$\frac{1}{\tan \alpha} = (0.62 - 0.41j + 0.13j^2)(E_1/E_2)^{0.59}(r/h)^{-0.11} + (0.43 - 0.52j + 0.19j^2)(E_1/E_2)^{0.5}(r/h)^{1.74} \log(N)$$

# Model Calibration

## Design Charts (based on laboratory test results)



# Design Procedure

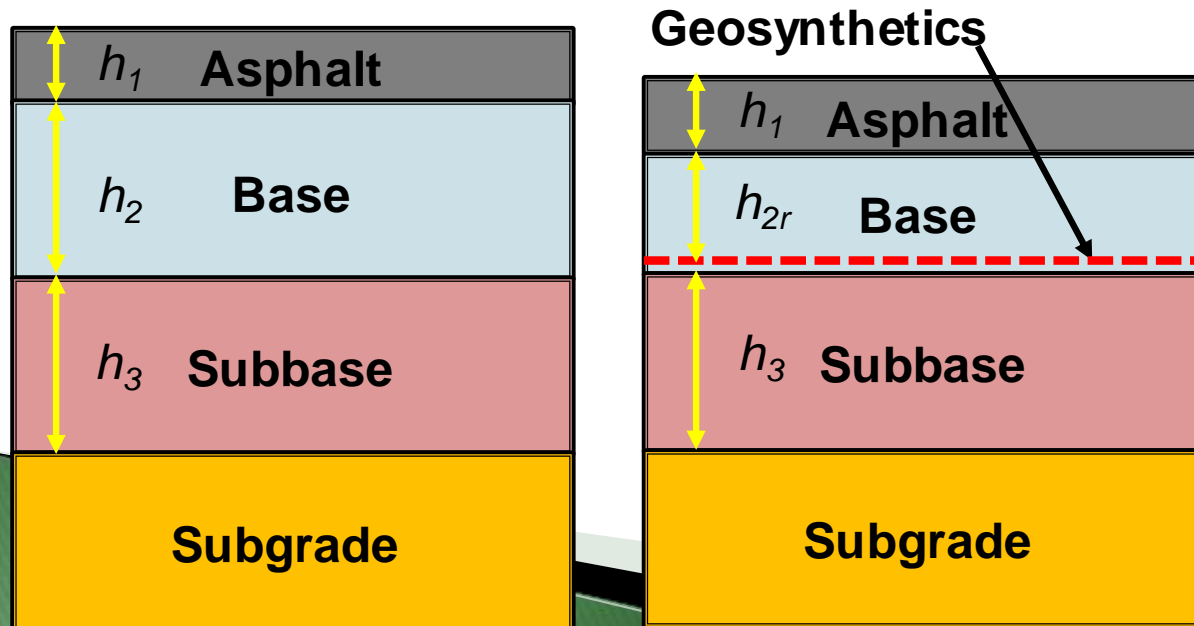
## Structural Design of Pavement

- ❑ Design methods for reinforced unpaved road
- ❑ Design methods for reinforced paved road (modified AASHTO)

For unreinforced road section,  $SN_U = a_1h_1 + a_2h_2 + a_3h_3 \dots\dots\dots (1)$

For reinforced road section,  $SN_U = a_1h_1 + a_{2r}h_{2r} + a_3h_3 \dots\dots\dots (2)$

From equation 1 & 2,  $a_{2r} = a_2 \times (h_2/h_{2r}) = a_2 \times BCR$



$a_1, a_2, a_3 =$  layer coefficients of asphalt, base, and subbase layer

$h_1, h_2, h_3 =$  thicknesses of asphalt, base, and subbase layer

$a_{2R}, h_{2R} =$  layer coefficient and thickness of the reinforced base layer

$SN_U =$  Structural number of the unreinforced roads

$BCR =$  Base course reduction factor

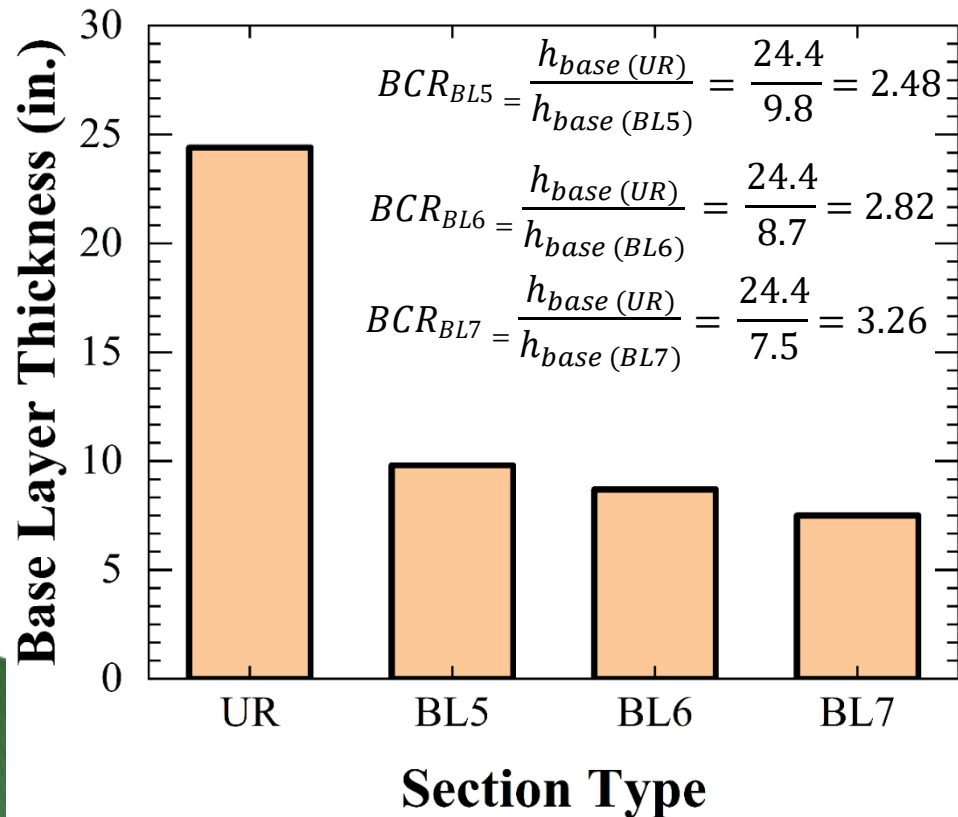
# Design Procedure

## BCR and Layer Coefficients for IFI Products

**Reinforced Unpaved road:** 
$$h_{base (R)} = \frac{SN_u - (a \times h)_{subbase}}{BCR (a)_{base}}$$

**Unreinforced Unpaved road:** 
$$h_{base (UR)} = \frac{SN_u - (a \times h)_{subbase}}{(a)_{base}}$$

**Base Course Reduction (BCR):** 
$$BCR = \frac{h_{base (UR)}}{h_{base (R)}}$$



### Layer coefficients:

$$a_{BL5} = BCR_{BL5} \times a_{UR} = 2.29 \times 0.14 = 0.32$$

$$a_{BL6} = BCR_{BL6} \times a_{UR} = 2.60 \times 0.14 = 0.36$$

$$a_{BL7} = BCR_{BL7} \times a_{UR} = 2.95 \times 0.14 = 0.41$$

Note:

The results presented here are based on laboratory test results and we still need to validate our findings based on full-scale field studies.



# Design Procedure

## Table for Layer Coefficients (allowable settlement 38 mm)

- Layer coefficients → increases with the stiffness of geosynthetics
- Layer coefficients → decreases with the increase of subgrade stiffness

Subgrade CBR	$j = 0.8$				$j = 0.98$				$j = 1.5$			
	N=10	N=100	N=1000	N=10000	N=10	N=100	N=1000	N=10000	N=10	N=100	N=1000	N=10000
0.25	0.37	0.37	0.37	0.37	0.41	0.41	0.41	0.40	0.48	0.48	0.48	0.47
0.50	0.38	0.38	0.37	0.37	0.42	0.42	0.41	0.41	0.49	0.49	0.48	0.48
0.75	0.39	0.38	0.37	0.37	0.43	0.42	0.41	0.41	0.50	0.49	0.48	0.47
1.00	0.39	0.38	0.37	0.36	0.43	0.42	0.41	0.40	0.51	0.49	0.47	0.46
1.25	0.39	0.37	0.36	0.35	0.44	0.42	0.40	0.39	0.51	0.48	0.46	0.45
1.50	0.39	0.37	0.35	0.35	0.44	0.41	0.39	0.38	0.51	0.47	0.45	0.44
1.75	0.39	0.36	0.35	0.34	0.44	0.40	0.39	0.38	0.50	0.46	0.44	0.43
2.00	0.39	0.36	0.34	0.34	0.43	0.40	0.38	0.37	0.49	0.46	0.44	0.42
2.25	0.38	0.36	0.34	0.33	0.43	0.40	0.38	0.37	0.49	0.45	0.43	0.42
2.50	0.38	0.35	0.34	0.33	0.42	0.39	0.38	0.37	0.48	0.45	0.43	0.42
2.75	0.38	0.35	0.34	0.33	0.42	0.39	0.38	0.37	0.48	0.44	0.43	0.42
3.00	0.38	0.35	0.34	0.34	0.42	0.39	0.38	0.37	0.47	0.44	0.43	0.42

# Summary

- Geosynthetic reduced the vertical stress on subgrade **by 20 to 80%**
- Vertical stress distribution angle after 5000 cycles: **UR < GG < GC < GG+GC**
- For very soft soil, geogrid reinforced section reduced the permanent deformation (PD) by **1.5 to 2.0 times**
- Geocell reinforced section reduced the PD by **3 to 4 times**
- Inclusion of geogrid with geocell decreased the PD by only **5-10%**
- G-H equation has been updated to include stiffer geogrids
- Design charts were developed to assist future design with IFI products

# LIFE FORMS

**Project: Design and Testing of IFI Geosynthetic Products**

**Number: 7**



# Performance of pavement sections with wicking geosynthetics

**Project Leader:** Nripojyoti Biswas

**Team members:** Krishneswar Ramineni and Avinash Gonnabathula

**PI:** Anand J. Puppala

Professor | A.P. and Florence Wiley Chair

Director – Center for Infrastructure Renewal

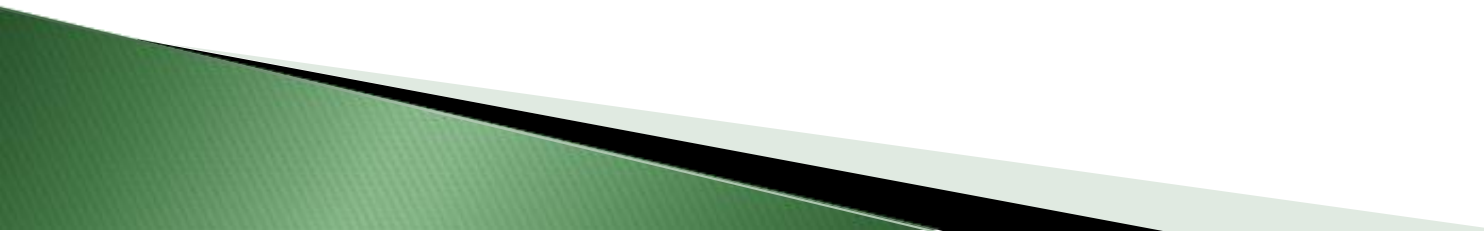
Closed Meeting

TAMU Site Proprietary

NSF IUCRC CICI TAMU SITE  
NSF IUCRC CICI - IAB Spring 2023 Meeting

May 8-9, 2023

# Presentation Outline

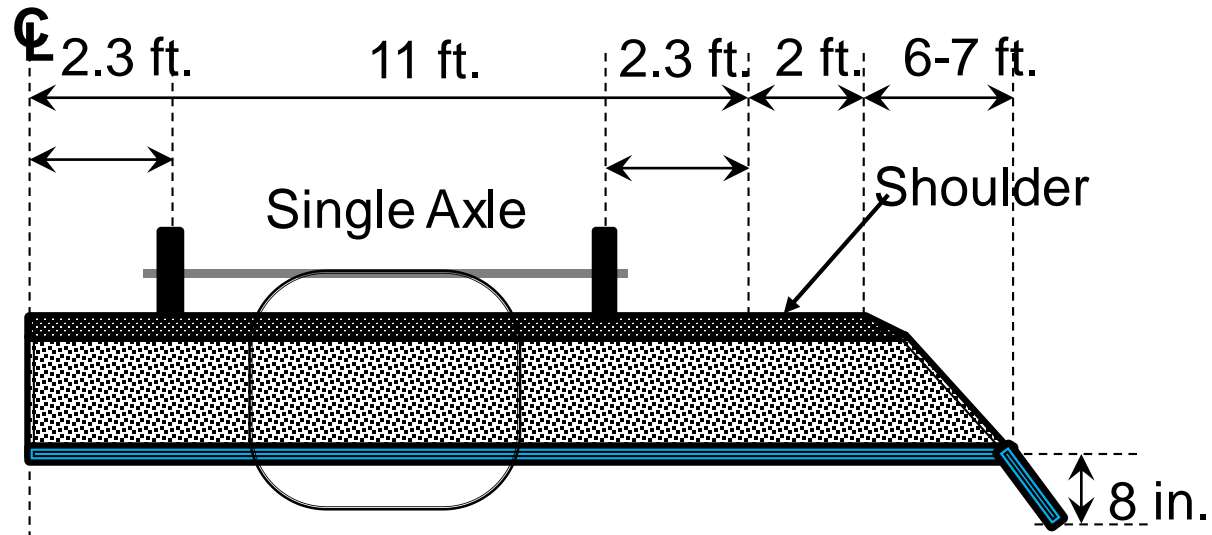
- ❖ Introduction
  - ❖ Field Test Sections- H<sub>2</sub>Ri Geosynthetics
  - ❖ Construction of H<sub>2</sub>Ri Pavement Sections
  - ❖ H<sub>2</sub>Ri Geosynthetics - Completed Tasks
  - ❖ H<sub>2</sub>Ri Geosynthetics - LCCA
  - ❖ Field Test Sections- RS580i Geosynthetics
  - ❖ Falling Weight Deflectometer (FWD) Test
  - ❖ Field Observations - RS580i section with RAP
  - ❖ Conclusions
- 

# Introduction

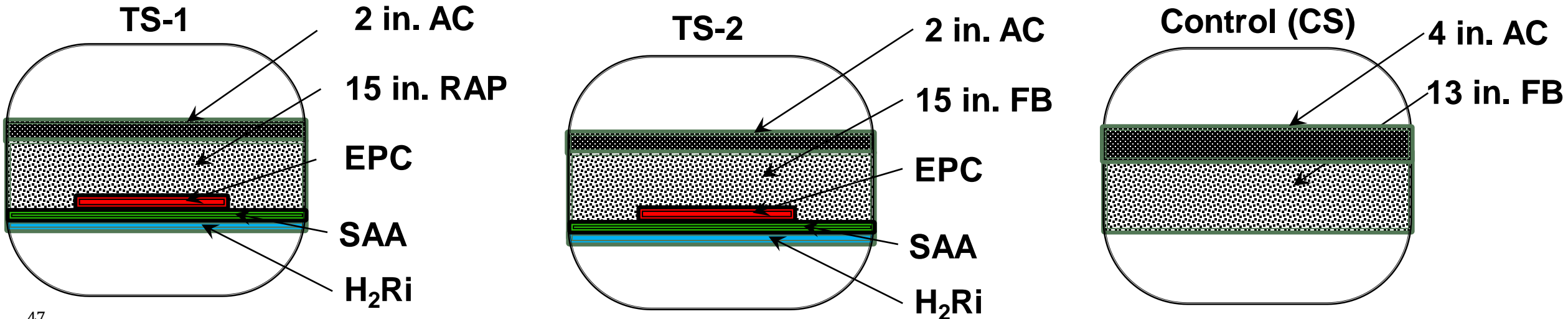
## ❖ Objective

- ❑ Evaluate the feasibility/efficiency of using wicking geosynthetic for improving drainage and strength of pavement sections built on high-plastic expansive soil
  
- ❖ Field Studies indicated efficacy of application
- ❖ Non-destructive tests showed sections performed remarkably well
- ❖ Laboratory studies provided evidence of improvements
- ❖ Preliminary sustainability analyses shows need for more robust study
- ❖ Potential to use similar novel geotextiles in the future?

# Field Test Sections- H<sub>2</sub>Ri Geosynthetics



AC – Asphalt Concrete RAP - Reclaimed Asphalt Pavement Aggregates FB - Flex Base  
 EPC - Earth Pressure Cells SAA - Shape Array Sensors



# Construction of H<sub>2</sub>Ri Pavement Sections



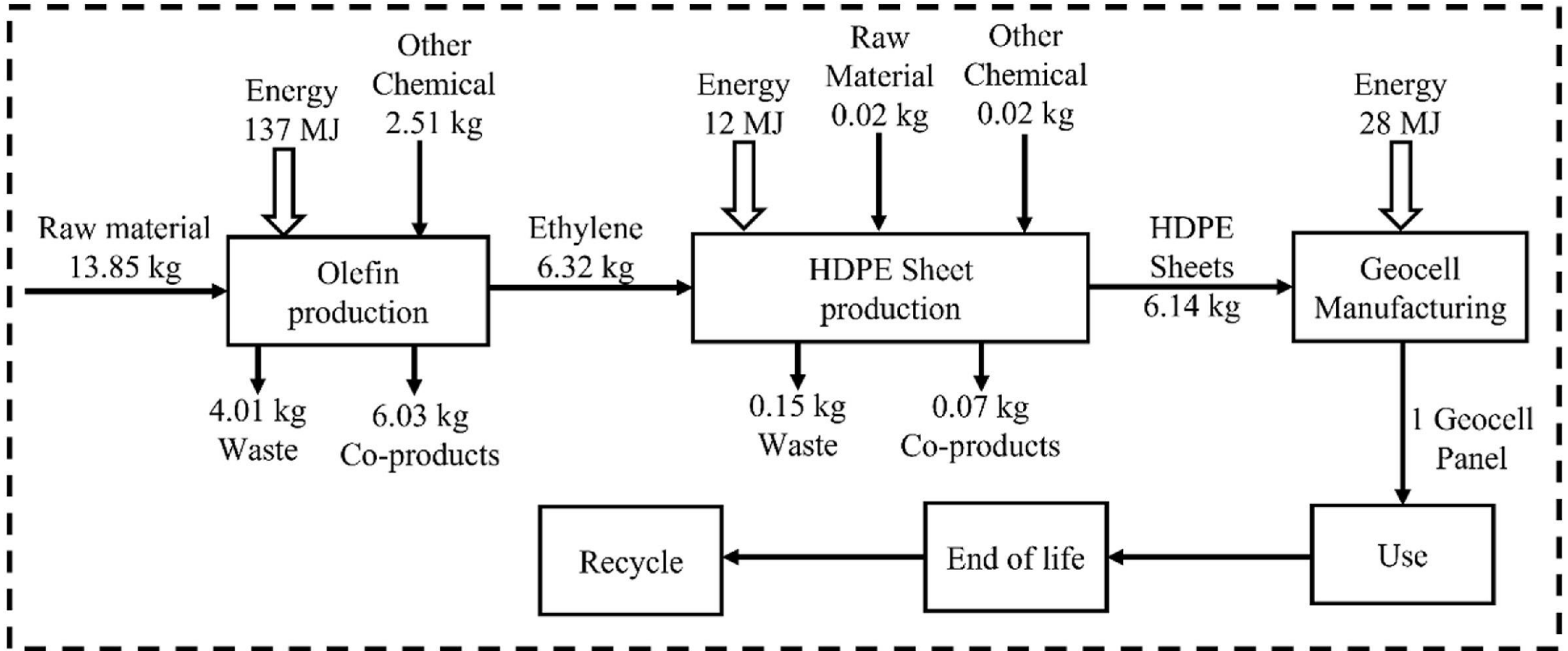


## H<sub>2</sub>Ri Geosynthetics – Completed Tasks

- ❖ Results from in-situ monitoring of test sections shows benefits of wicking fibers (**Dec 2020 and May 2021 meeting**)
- ❖ Non-destructive tests using APLT and FWD provided benefits of geosynthetic layer as compared to unreinforced layers (**Dec 2021 meeting**)
- ❖ Benefits of application of the novel gtx were verified using laboratory studies (**May 2022 meeting**)
- ❖ Preliminary sustainability assessment indicates GHG emissions during production of geotextile and cost of geotextile are major factors affecting sustainability benefits of the project (**Dec 2022 meeting**)
- ❖ **Need to develop a comprehensive Life Cycle Cost Analysis (LCCA) for the H2Ri geotextile (cradle-to-gate + End-of-life)**
- ❖ **Investigate benefits of other similar geosynthetic products..**

# H<sub>2</sub>Ri Geosynthetics - LCCA

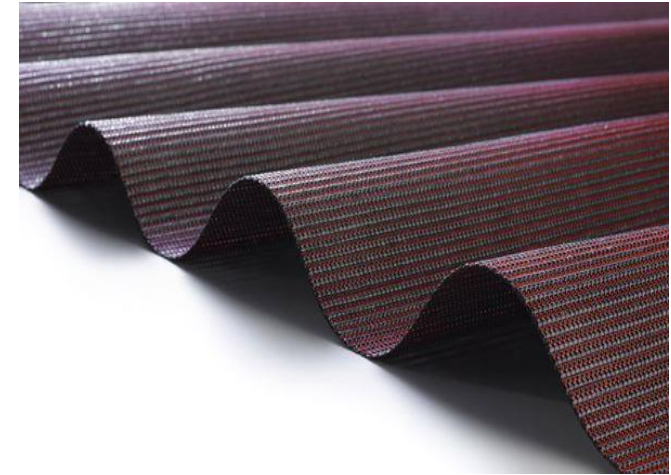
Khan and Puppala 2023



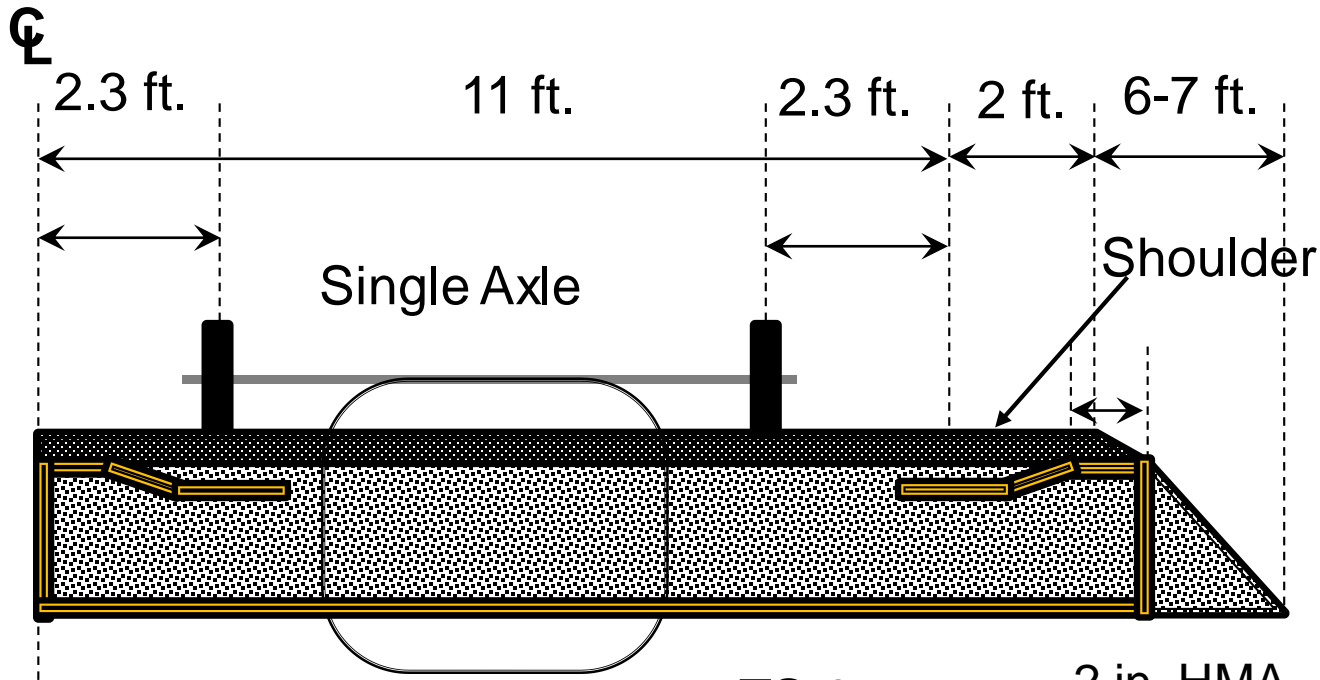
❖ **Similar Life Cycle Cost Analysis (LCCA) for the H<sub>2</sub>Ri geotextile (cradle-to-gate + End-of-life)**

# Field Test Sections- RS580i Geosynthetics

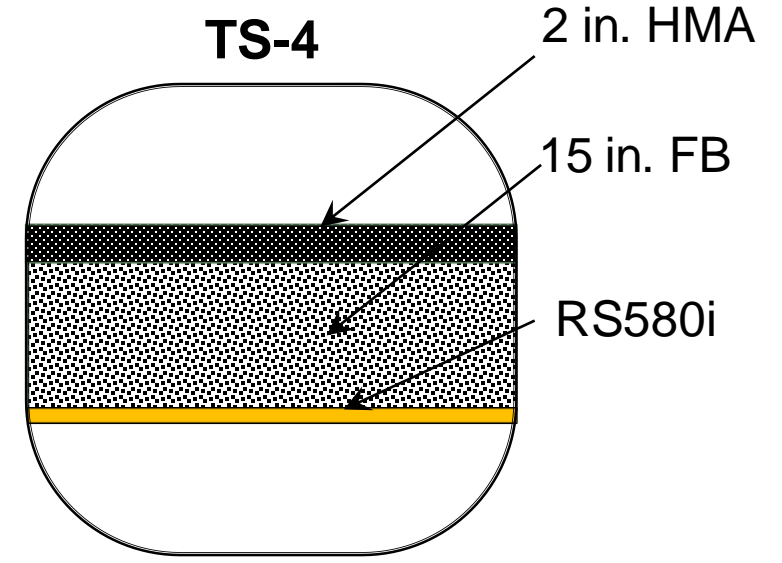
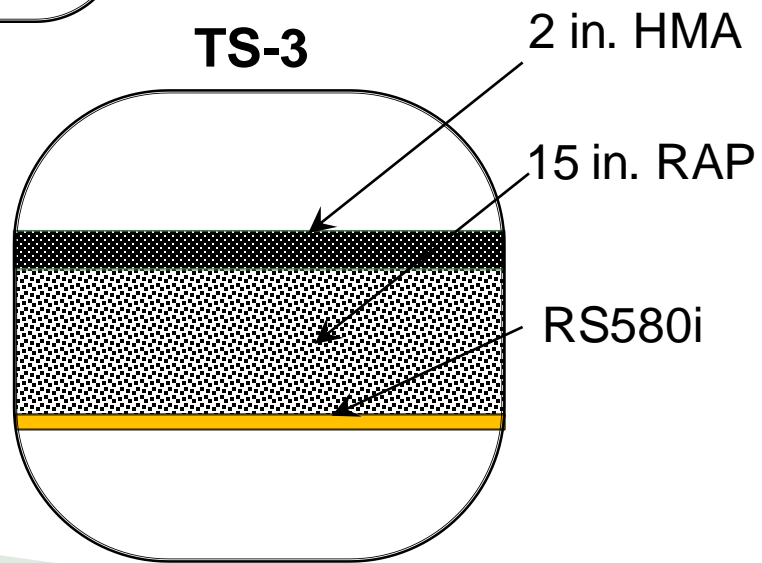
- ❖ Higher tensile strength and modulus
- ❖ Good soil and base layer confinement
- ❖ Provides superior filtration and separation



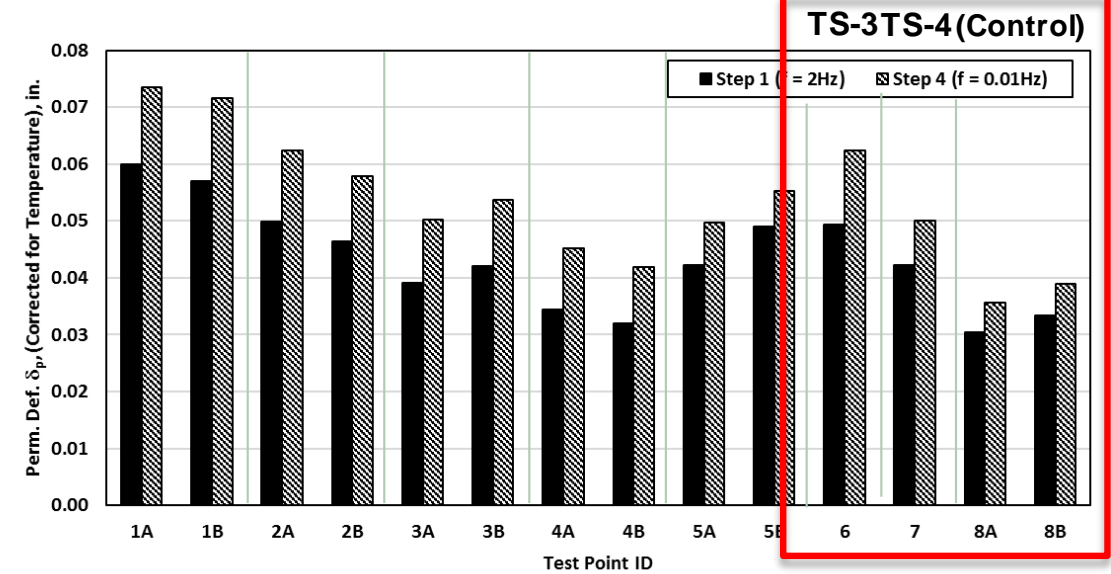
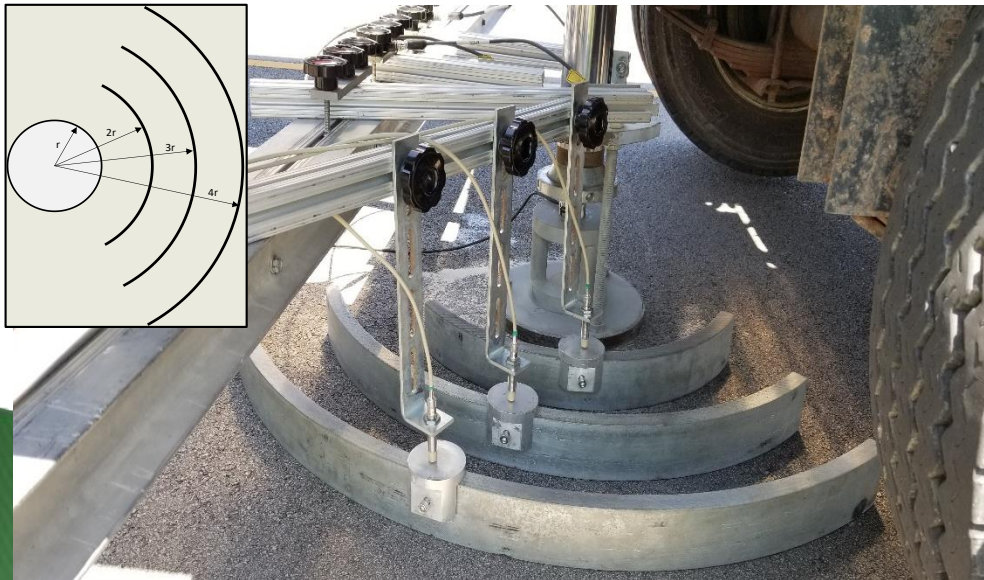
# Field Test Sections- RS580i Geosynthetics



**AC** – Asphalt Concrete  
**RAP** – Reclaimed Asphalt Pavement Aggregates  
**FB** – Flex Base  
**EPC** – Earth Pressure Cells  
**SAA** – Shape Array Sensors

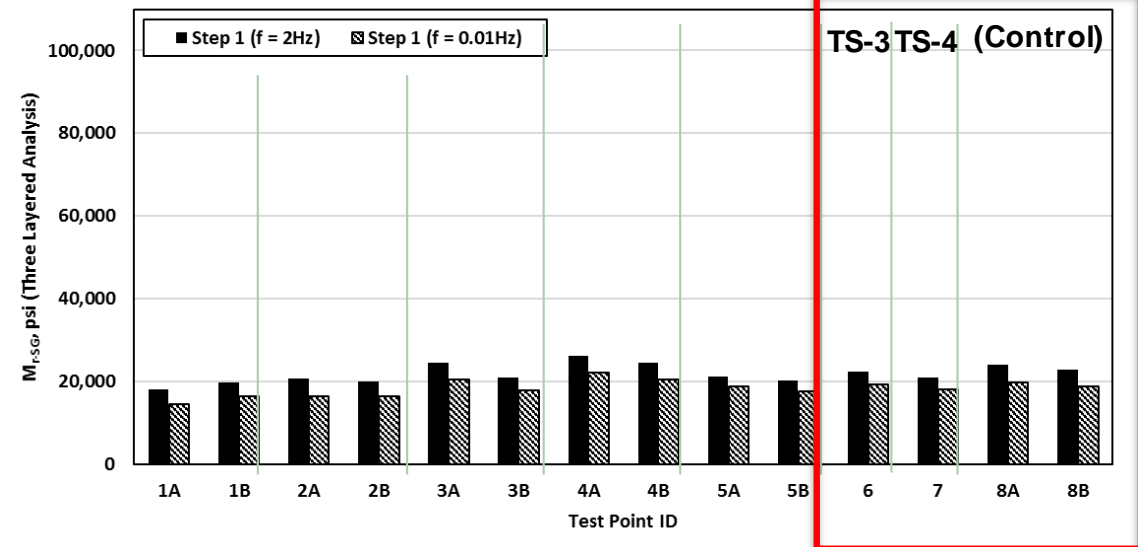


# Automated Plate Load Testing (APLT)



Permanent deformation  $\delta_p$  at the end of first step 1 (100 cycles) at end of Step 4 at each test location

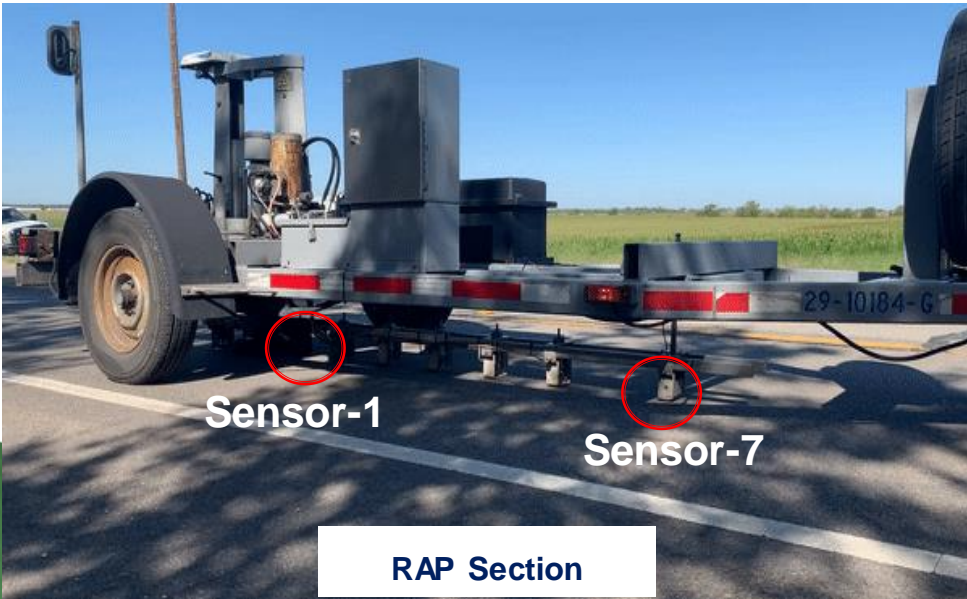
TS-4 and TS-5 showed more permanent deformation



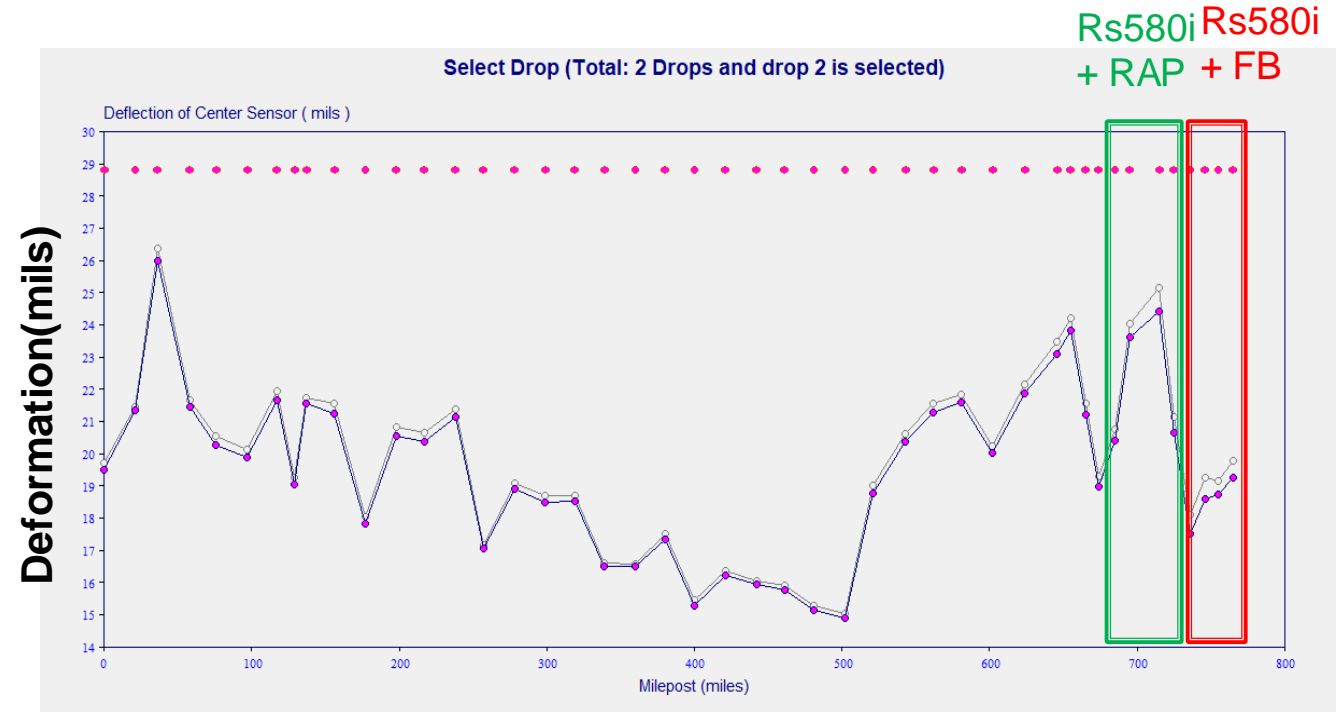
Back-calculated  $M_{r-SG}$  at the end of first step 1 (100 cycles) and end of Step 4 at each test location

TS-4 and TS-5 showed similar Resilient Modulus

# Falling Weight Deflectometer (FWD) Test



1 mils = 0.001 in.



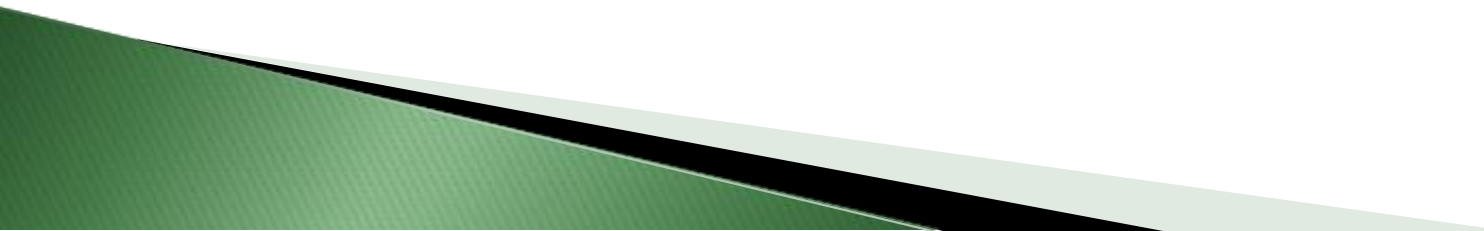
❖ Deformation of RS580i+RAP section was significant

# Field Observations - RS580i section with RAP



- ❖ Deformation of RS580i + RAP section was more than other sections
- ❖ Need for novel RS580i series for better performance
- ❖ **Future research need – New series of RS580 with wicking abilities**

# Conclusions

- ❖ **Wicking geotextile is beneficial for reinforcing pavements built on expansive soils**
  - ❖ **Need a robust LCCA framework to realize the potential of the sustainable benefit of these novel geosynthetics**
  - ❖ **Construction of test sections with RS580i (non-wicking geosynthetic) to analyze the new “burrito-type” design benefit**
  - ❖ **RS580i+RAP do not provide long-term beneficial performance**
  - ❖ **RS580i+RAP section has maximum resilient and permanent deformation**
  - ❖ **New series of RS580 with wicking fibers could be beneficial**
- 



# LIFE FORMS

**Project: Performance of pavement sections with wicking geosynthetics**

**Number: 8**

